PALEOCEANOGRAPHY, VOL. 7, NO. 3, PAGES 251-272, JUNE 1992

PALEOPRODUCTIVITY AND CARBON BURIAL ACROSS THE CALIFORNIA CURRENT: THE MULTITRACERS TRANSECT, 42°N

Mitchell Lyle,[1] Rainer Zahn,[2] Frederick Prahl,[3] Jack Dymond,[3] Robert Collier,[3] Nicklas Pisias,[3] and Erwin Suess[2]

Abstract. The Multitracers Experiment studied a transect of water column, sediment trap, and sediment data taken across the California Current to develop quantitative methods for hindcasting paleoproductivity. The experiment used three sediment trap moorings located 120 km, 270 km, and 630 km from shore at the Oregon/California border in North America. We report here about the sedimentation and burial of particulate organic carbon (C_{org}) and $CaCO_3$. In order to observe how the integrated $CaCO_3$ and C_{org} burial across the transect has changed since the last glacial maximum, we have correlated core from the three sites using time scales constrained by both radiocarbon and oxygen isotopes. By comparing surface sediments to a two-and-a-half year sediment trap record, we have also defined the modern preservation rates for many of the labile sedimentary materials. Our analysis of the C_{org} data indicates that significant amounts (20-40%) of the total C_{org} being buried today in surface sediments is terrestrial. At the last glacial maximum, the terrestrial C_{org} fraction within 300 km of the coast was about twice as large. Such large fluxes of terrestrial C_{org} obscure the marine C_{org} record, which can be interpreted as productivity. When we corrected for the terrestrial organic matter, we found that the mass accumulation rate of marine C_{org} roughly doubled from the glacial maximum to the present. Because preservation rates of organic carbon are high in the high sedimentation rate cores, corrections for degradation are straightforward and we can be confident that organic carbon rain rate (new productivity) also doubled. As confirmation, the highest burial fluxes of other biogenic components (opal and Ba) also occur in the Holocene. Productivity off Oregon has thus increased dramatically since the last glacial maximum. $CaCO_3$ fluxes also changed radically through the deglaciation; however, they are linked not to $CaCO_3$ production but rather to changes in deepwater carbonate chemistry between 18 Ka and now.

INTRODUCTION

The Multitracers Project was designed to study how the annual oceanographic cycle affects the production of biogenic sedimentary components and how productivity information is preserved in the sediments. We studied multiple paleoproductivity tracers, both geochemical and micropaleontological, to peel away the diagenetic changes obscuring the sedimentary record and to reconstruct the evolution of primary productivity in the northern California Current since the last glacial maximum. Along the transect, we have defined hydrographic conditions, collected falling particles with sediment traps, and investigated standing stocks of microfossil-forming zooplankton with plankton tows. We have also assessed modern sedimentary geochemical conditions with pore water studies, and our collaborators are studying radiochemical fluxes, phytoplankton fluxes, standing stocks of certain organic geochemical biomarkers, and primary productivity. To determine how productivity off coastal Oregon and northern California has been affected by the waning of the great Pleistocene ice sheets we have also investigated the burial fluxes, or mass accumulation rates (MARs), of the geochemical and micropaleontological tracers. This paper will focus upon the sedimentary C_{org} record and the implications this record has for paleoproductivity. Other syntheses combine these studies with microfossil data and the other geochemical tracers [e.g., Sancetta et al., 1992; Welling, 1991].

[1]Borehole Research Group, Lamont-Doherty Geological Observatory, Palisades, New York.

[2]GEOMAR, Kiel, Germany.

[3]College of Oceanography, Oregon State University, Corvallis.

Paper number 92PA00696.
0883-8305/92/92PA-00696$10.00

METHODS

C_{org} and $CaCO_3$ analyses were performed by the acidification/wet oxidation method described by Weliky et al.[1983] with modifications described by Lyle et al.,[1988]. Opal was analyzed by Na_2CO_3 digestion and Atomic Absorption Spectrophotometry (AAS) analysis of Si [Lyle et al., 1988]. Inorganic chemical analyses in the sediments were done partly by Instrumental Neutron Activation Analysis (INAA) following techniques described by Laul [1979], and partly by X-ray flourescense (XRF), as described by Finney et al., [1988]. We used the procedure described by Prahl et al., [1989a] for analysis of the "free" lipid fraction in the sediments.

Oxygen isotope analyses were performed using the OSU Finnigan MAT 251 isotope ratio mass spectrometer coupled online to an Autoprep Systems automated "common acid-bath" $CaCO_3$ preparation device. Calibration to the PDB $CaCO_3$ standard scale was done through National Bureau of Standards (NBS)19 and NBS 20 standards. Reproducibility for $\delta^{18}O$ and $\delta^{13}C$ is 0.09 and 0.04 o/oo ($\pm 1\sigma$) respectively. The isotope measurements were carried out on benthic foraminifers C. wuellerstorfii and Uvigerina spp. (U. peregrina and U. senticosa). All oxygen isotope data are referred to the Uvigerina scale by adding 0.64 o/oo to the C. wuellerstorfi values [Shackleton, 1974].

DESCRIPTION OF THE MULTITRACERS TRANSECT

Oceanographic setting: The California Current is one of the world's important eastern boundary currents. The current annually carries about 10 Sv of cold, low salinity, North Pacific water into the eastern tropical Pacific (Figure 1) [Sverdrup et al., 1942; Hickey, 1979]. It is the major transport mechanism to remove fresh water from the North Pacific. Coastal upwelling driven by persistent summer northerly winds is also associated with the California Current. Centers of upwelling off Oregon, California, and Mexico add cold, but more saline, water to the southward flowing current. The California Current combines diffuse flow, which extends many hundreds of kilometers from the coast, with local high-velocity zones of southward flow near the coast [e.g., Huyer et al., 1991]. The core of the offshore California Current flow is located approximately 250-350 km from the coast at the border of Oregon and California and is about 300 km from the coast at Point Conception [Hickey, 1979; Lynn and Simpson, 1987].

The California Current is subject both to seasonal and to interannual cycles. The pattern of winds along the coast controls seasonal variations. Changes in the dynamic topography of the North Pacific Gyre produce interannual variability in the current. Modeling studies [Pares-Sierra and O'Brien, 1989] have indicated that the local wind field in the northeastern Pacific is adequate to drive the annual cycle of the current and to create the general features of its structure. Interannual variations of the current could only be modeled, however, by coupling the local model with one driven by equatorial winds. Kelvin waves generated during El Niño/Southern Oscillation (ENSO) events in the equatorial Pacific propagate up the western coast of North America and strongly affect the California Current. Thus the current structure reflects both local winds along the west coast of the United States and basin-wide events within the North and equatorial Pacific Ocean.

The modeling suggests that in the much longer climatic cycles that are observable by paleoceanographic studies, the location and strength of both trade winds and westerlies should probably have a major impact on mean transport in the California Current. A shift in the position of the North Pacific High at the last glacial maximum, as predicted by Kutzbach [1987], should also strongly affect the structure of the California Current flow as well as the locations of maximum coastal upwelling.

Our 42°N transect off Cape Blanco (Figure 2) exhibits strong northerly winds during the summer and strong southwesterly winds during the winter [Nelson, 1977]. This annual cycle produces the most pronounced seasonality of surface circulation in the California Current system. Southward flow typically peaks between 250 to 350 km offshore the Oregon coast during the late summer or early fall. Near the coast, a seasonal cycle in southward flow also occurs, but it peaks in the spring or early summer [Hickey, 1979]. Coastal upwelling is an important feature of this system [Huyer, 1983] and, as expected from the seasonal nature of the northerly winds along the coast, the intensity of upwelling follows a seasonal cycle with a maximum in August [Landry et al., 1989]. Upwelling is evident hundreds of kilometers offshore, as eddies, meanders, or "jets" of cold surface waters flow out from prominent coastal headlands, such as Cape Blanco [Ikeda and Emery, 1984].

Geologic setting: The Multitracers Transect crosses the Gorda Ridge, a slowly spreading mid-ocean ridge between the Mendocino and Blanco Fracture Zones [Riddihough, 1980; Stoddard, 1987] (Figure 2). The transect was chosen at 42° N partly because the topographic swell of the Gorda Ridge directed major Pleistocene turbidites elsewhere, into basins surrounding the ridge. Sediments on the Gorda Ridge are

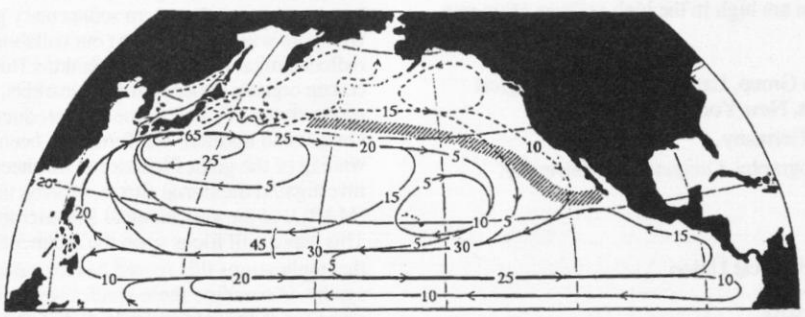

Fig. 1. Water transport in north Pacific [after Sverdrup, et al., 1942]. Units are in Sverdrups (10^6 m^3/s). Dashed lines mark cold currents.

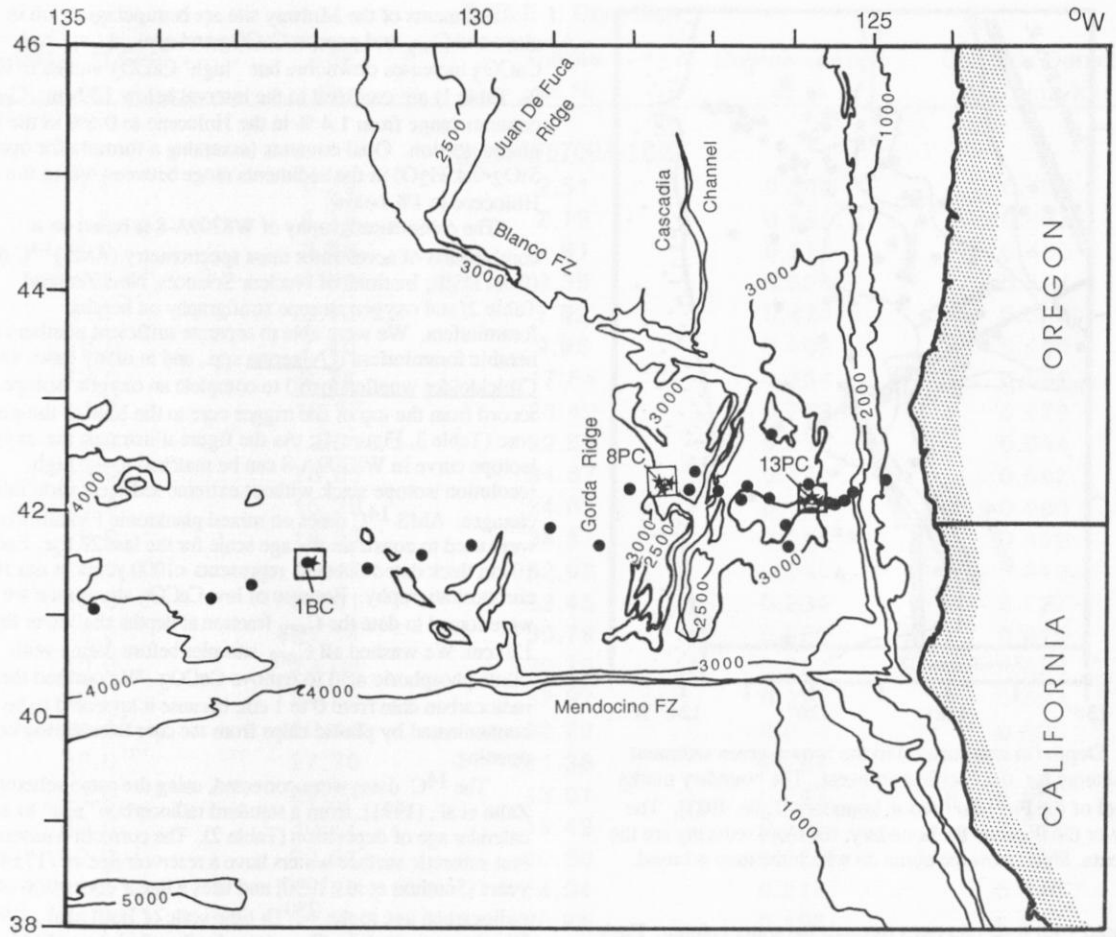

Fig. 2. Bathymetry along the Multitracers Transect with piston core locations (stars), gravity core locations (circles), and mooring sites (open squares). The core W8709A-1BC is from the Gyre Site, W8709A-8PC is from the Midway Site, and W8709A-13PC is from the Nearshore Site.

hemipelagic, while most sediments deeper than 3100 m near the Gorda Ridge have the flat-lying, highly reflective seismic characteristics of turbidites [Dehlinger et al., 1971]. The region around the Gyre mooring site was also protected from the Pleistocene turbidites by another subtle northwest trending bathymetric high and an associated chain of seamounts.

The sedimentary redox environment, important for the preservation of many paleoproductivity tracers, is determined by the rain rate of reactive organic matter to the seafloor. It can be depicted semiquantitatively by mapping the depth in sediment cores to the brown-green, or Fe^{III}-Fe^{II}, boundary (Figure 3); [Lyle, 1983]. From the Oregon/northern California coast out to the longitude of the Gorda Ridge (about 127°W) this boundary occurs within 1 cm of the seafloor, reflecting high C_{org} deposition. On the west flank of the ridge it plunges to deeper than 20 cm. North of the Blanco Fracture Zone (43°-44°N) a bulge of more reducing sediments (shallow brown-green boundary) follows the Cascadia Channel caused by the transport of C_{org} from the shelf to the Cascadia Basin by Holocene turbidity currents from the Astoria Fan.

Mooring locations: The sites in the transect, located between the Mendocino and Blanco Fracture Zones, cross large gradients in primary productivity, particle fluxes, and resulting sediment accumulation. The high seasonal oceanographic variability also contributes a large dynamic range for the calibrations of tracers to fluxes. The transect extends from North America at the California-Oregon border to about 1000 km offshore (Figure 2) and was anchored by three mooring sites, known as Nearshore (42° 05'N, 125°45'W, 2829-m water depth; 120 km from shore), Midway (42°10'N, 127°35'W, 2830-m water depth; 270 km from shore), and Gyre (41°30'N, 132°W, 3664-m water depth; 630 km from shore). Each mooring had an array of sediment traps nominally at 500 m, 1000 m, 1500 m, and 1750 m below the sea surface, and a trap 500 m above the seafloor. These sediment trap moorings were first emplaced in September, 1987, and were maintained until the fall of 1991. The sediment traps collected a time series of particle flux in sampling cups that changed automatically at bimonthly to biweekly time intervals. We also collected a series of sediment cores along the Transect (Figure 2) and have occupied hydrographic stations between mooring sites.

SEDIMENT RECORDS

In this paper, we present data from each of the mooring sites. Sedimentary mass accumulation rates (MARs) of different components have been measured downcore and are

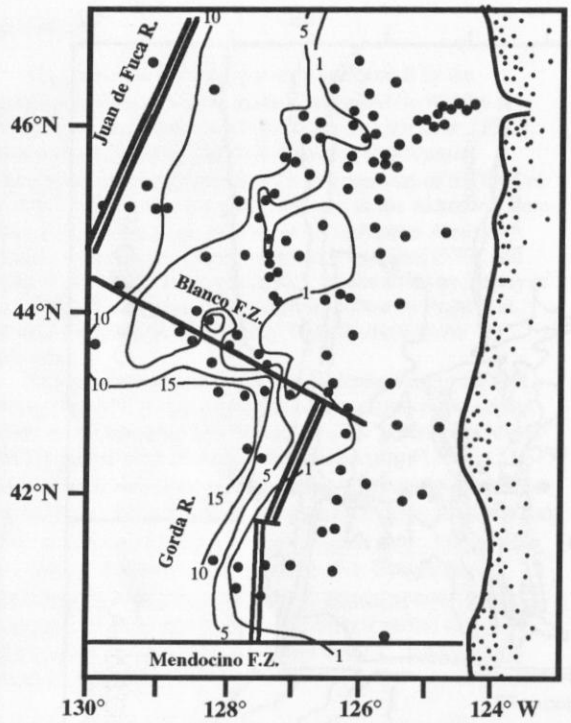

Fig. 3. Depth (in centimeters) to the brown-green sediment color change for the Pacific northwest. The boundary marks the level of the Fe^{III}/Fe^{II} redox boundary [Lyle, 1983]. The shallower the depth to the boundary, the more reducing are the sediments. Dots show the cores on which the map is based.

compared with their rain rates through the water column. Each core or piston/trigger weight pair we studied preserves surface sediments and extends through the last glacial maximum. For the Gyre mooring site we used a box core, while for the Nearshore and Midway sites we spliced together records from a piston core and its corresponding trigger core.

Gyre (W8709A-1BC; 41°32.54'N, 131°57.33'W, 3680 m): The core has low $CaCO_3$ at the surface, but below 15 cm has abundances greater than 15% (Table 1). C_{org} contents are low, averaging 0.3%. We established a sedimentation rate for this core, based upon oxygen isotope stratigraphy of Uvigerina spp. benthic foraminifera, of 1.3 cm/kyr. We have neither a record long enough nor a sedimentation rate high enough to establish sedimentation rate changes within this core. The sedimentation rate for much of the Pleistocene must have been lower than this, however, because the Brunhes-Matuyama magnetic reversal boundary (730 Ka) is at 530 cm in a nearby piston core (W8709A-2PC) (R. Karlin, personal communication, 1988).

Midway (W8709A-8PC and 8TC; 42°15.74'N, 127°40.68'W, 3111 m): W8709A-8 is 875 cm long and was spliced with its 190 cm-long, 10-cm diameter trigger core. The upper brown layer was approximately the same thickness (10 cm) in the trigger core as in nearby box cores, so we believe that little or no surface material was lost during coring. On the basis of comparison of magnetic susceptibility and $CaCO_3$ records between the trigger and the piston cores, the piston core overpenetrated by 140 cm. The spliced record (a total of 1015 cm) reaches oxygen isotope stage 5A.

Sediments of the Midway site are hemipelagic, rich in clays and C_{org} and poor in $CaCO_3$ and opal. As at Gyre, $CaCO_3$ increases downcore but "high" $CaCO_3$ values (>10 wt %, Table 1) are confined to the interval below 120 cm. C_{org} contents range from 1.4 % in the Holocene to 0.6% in the late glacial section. Opal contents (assuming a formula for opal of $SiO_2 \cdot 0.45H_2O$) in the sediments range between 6% in the Holocene to 1% below.

The chronostratigraphy of W8709A-8 is based on a combination of accelerator mass spectrometry (AMS) ^{14}C dates (from DSIR, Institute of Nuclear Sciences, New Zealand, Table 2) and oxygen isotope stratigraphy on benthic foraminifera. We were able to separate sufficient numbers of benthic foraminifera (Uvigerina spp., and in many cases also Cibicidoides wuellerstorfii) to complete an oxygen isotope record from the top of the trigger core to the base of the piston core (Table 3, Figure 4). As the figure illustrates, the oxygen isotope curve in W8709A-8 can be matched to the high-resolution isotope stack without extreme sedimentation rate changes. AMS ^{14}C dates on mixed planktonic foraminifera were used to constrain the age scale for the last 23 kyr. Each 5-10 cm thick dated interval represents <1000 years in our final chronostratigraphy. Because of low $CaCO_3$ abundance we were forced to date the C_{org} fraction at depths shallower than 120 cm. We washed all C_{org} samples before dating with dilute phosphoric acid to remove $CaCO_3$. We omitted the radiocarbon date from 0 to 1 cm, because it appeared to be contaminated by plastic chips from the core liner during core opening.

The ^{14}C dates were corrected, using the same scheme as Zahn et al , [1991], from a standard radiocarbon "age" to a calendar age of deposition (Table 2). The correction assumes that subarctic surface waters have a reservoir age of 717±47 years [Southon et al., 1990] and uses a linear correction of the radiocarbon age to the ^{230}Th time scale of Bard et al , [1990]. We also corrected the C_{org} dates for the admixture of old, presumably terrestrial, C_{org} in the sediment by subtracting the age of planktonic foraminifera at 120-130 cm from the C_{org} date at 125-126 cm. The difference, 4300 years, was then subtracted from the other C_{org} dates. When this correction is applied, the dates follow a smooth age-depth relationship. We fit ^{14}C ages with a third order curve for calculation of sedimentation rates and MARs for the last 23 kyr and linked the radiocarbon-based time scale to the oxygen isotope-based time scale prior to 23 Ka by minor adjustments of the oxygen isotope ages.

Nearshore (W8709A-13PC and 13TC; 42°07.01'N, 125°45.00'W, 2712 m): W8709A-13 is a piston core, 872 cm long, joined with a trigger core, 235 cm long, that was taken on top of a ridge 400 m above the nearby turbidite basin. The sediments are hemipelagic but are poorer in $CaCO_3$ and richer in opal and C_{org} than cores to the west. Holocene sediments contain up to 12% opal, 2% C_{org}, and as little as 0.8% $CaCO_3$. In contrast, the Pleistocene section has opal contents are as low as 2%, C_{org} as low as 0.8%, and $CaCO_3$ as high as 9%. Sedimentation rates are nearly double those in the Midway core and 15 times higher than the Gyre core.

Despite the core's location at the top of a 400-m high ridge, three small sand turbidites were found at 208 cm, 232 cm, and 256 cm (14 Ka, 15 Ka, and 16 Ka by our time scale). The upper two turbidites are ~2 cm thick, and the lower one is ~4 cm thick. They are probably thin overbank sands from three huge turbidites, not the bases of thick turbidite sequences.

TABLE 1. Core Data

Depth in Core cm	Age ka	Calcite wt %	Organic Carbon wt %	Dry Bulk Density* gm/cm2/kyr
		Gyre, W8709A-1BC		
0.5	0.39	2.51	0.563	0.458
1.5	1.16	2.19	0.555	0.487
4.0	3.08	2.81	0.516	0.480
6.0	4.62	3.35	0.550	0.491
8.0	6.16	7.92	0.470	0.529
10.0	7.70	9.98	0.402	0.550
12.0	9.24	17.84	0.334	0.589
14.0	10.77	28.40	0.272	0.670
16.0	12.31	32.55	0.213	0.644
18.0	13.85	34.87	0.178	0.692
20.0	15.39	34.67	0.192	0.680
22.0	16.93	34.87	0.215	0.652
24.0	18.47	32.93	0.246	0.642
26.0	20.01	33.45	0.234	0.627
28.0	21.54	30.76	0.380	0.616
30.0	23.08	30.79	0.227	0.620
32.0	24.62	32.37	0.227	0.634
34.0	26.16	32.72	0.276	0.593
36.0	27.70	21.38	0.264	0.570
38.0	29.24	13.01	0.247	0.559
40.0	30.77	19.42	0.201	0.548
42.0	32.31	10.08	0.215	0.556
44.0	33.85	14.94	0.214	0.540
46.0	35.39	20.88	0.195	0.541
48.0	36.93	16.22	0.195	0.547
		Midway, W8709A-8TC		
0.5	0.04	1.09	1.299	0.315
3.5	0.30	2.19	1.363	0.369
6.5	0.56	2.68	1.387	0.353
10.5	0.91	2.95	1.305	0.345
15.5	1.37	2.44	1.245	0.362
20.5	1.83	2.66	1.216	0.380
25.5	2.30	2.58	1.215	0.397
30.5	2.78	2.45	1.168	0.403
35.5	3.27	2.73	1.109	0.415
40.5	3.77	2.98	1.103	0.399
45.5	4.28	3.16	1.135	0.398
50.5	4.79	2.99	1.144	0.399
55.5	5.31	3.01	1.084	0.399
60.5	5.84	2.77	1.098	0.406
65.5	6.37	1.71	1.068	0.409
70.5	6.90	2.30	1.183	0.395
75.5	7.44	2.82	1.204	0.392
80.5	7.98	3.87	1.231	0.422
85.5	8.53	5.30	1.291	0.420
90.5	9.07	5.47	1.313	0.417

TABLE 1. (continued)

Depth in Core cm	Age ka	Calcite wt %	Organic Carbon wt %	Dry Bulk Density* gm/cm2/kyr
95.5	9.62	5.05	1.241	0.412
105.5	10.72	5.69	1.206	0.430
115.5	11.83	4.77	1.184	0.364
124.5	12.81	9.13	1.105	0.454
135.5	14.01	14.67	1.226	0.521
145.5	15.09	19.30	1.021	0.511
155.5	16.14	25.08	0.730	0.562
165.5	17.18	23.01	0.635	0.550
175.5	18.18	21.54	0.636	0.558
185.5	19.16	17.02	0.719	0.547
		Midway, W8709A-8PC		
12.5	15.83	19.44	0.890	0.399
22.5	16.87	24.07	0.630	0.487
32.5	17.88	21.64	0.610	0.496
42.5	18.87	20.60	0.650	0.507
52.5	19.82	15.67	0.630	0.549
62.5	20.73	10.18	0.660	0.613
72.5	21.60	13.34	0.670	0.504
82.5	22.42	12.17	0.740	0.583
92.5	23.18	13.08	0.690	0.565
102.5	23.89	11.10	0.640	0.496
113.5	24.68	12.19	0.580	0.554
123.5	25.39	11.64	0.660	0.537
132.5	26.04	9.80	0.700	0.566
142.5	26.75	9.03	0.760	0.454
152.5	27.46	6.38	0.710	0.547
162.5	28.18	11.44	0.700	0.581
172.5	28.89	10.65	0.680	0.462
182.5	29.61	7.48	0.750	0.466
192.5	30.32	9.46	0.770	0.459
200.5	30.94	11.25	0.730	0.494
211.5	31.78	10.07	0.790	0.494
221.5	32.55	15.85	0.760	0.494
231.5	33.32	18.38	0.770	0.494
241.5	34.09	9.49	0.920	0.494
251.5	34.92	11.16	0.910	0.494
261.5	35.76	6.47	0.800	0.494
271.5	36.59	8.17	0.860	0.494
281.5	37.42	8.75	0.880	0.494
291.5	38.26	8.33	0.860	0.494
301.5	39.09	9.05	0.900	0.494
321.0	40.72	13.07	0.750	0.494
341.0	42.32	9.06	0.850	0.494
361.0	43.92	10.38	0.760	0.494
381.0	45.52	15.45	0.740	0.494
401.0	47.12	17.93	0.740	0.494
421.0	48.72	13.81	0.820	0.494

TABLE 1. (continued)

Depth in Core cm	Age ka	Calcite wt %	Organic Carbon wt %	Dry Bulk Density* gm/cm2/kyr
441.0	50.32	13.16	0.750	0.494
461.0	52.32	15.59	0.830	0.494
481.0	55.17	10.73	0.770	0.494
501.0	58.03	6.58	0.770	0.494
		Nearshore, W8709A-13TC		
0.5	0.30	1.17	1.816	0.437
10.5	1.07	1.19	1.909	0.508
20.5	1.84	1.16	2.015	0.513
30.5	2.61	0.92	1.639	0.532
40.5	3.38	1.31	1.540	0.544
50.5	4.15	1.29	1.539	0.513
60.5	4.92	1.26	1.477	0.565
70.5	5.54	1.39	1.420	0.553
80.5	6.17	1.08	1.399	0.565
90.5	6.79	1.07	1.358	0.555
100.5	7.42	1.38	1.341	0.587
110.5	8.04	1.99	1.470	0.582
120.5	8.67	2.17	1.404	0.585
130.5	9.29	2.08	1.387	0.592
140.5	9.92	2.49	1.342	0.610
150.5	10.54	2.47	1.541	0.614
160.5	11.17	2.70	1.299	0.619
170.5	11.79	3.49	1.277	0.626
180.5	12.29	3.84	1.393	0.632
190.5	12.79	5.67	1.493	0.635
200.5	13.29	3.98	1.298	0.638
210.5	13.79	6.75	1.026	0.641
220.5	14.29	8.07	1.082	0.643
		Nearshore, W8709A-13PC		
2.5	4.60	0.79	1.550	0.388
12.5	5.07	1.07	1.380	0.463
22.5	5.53	0.80	1.240	0.528
32.5	6.00	0.48	1.300	0.510
42.5	6.47	0.74	1.280	0.541
52.5	6.93	0.97	1.350	0.552
62.5	7.40	1.46	1.380	0.513
72.5	7.86	1.94	1.390	0.539
82.5	8.33	2.24	1.340	0.548
92.5	8.79	2.00	1.400	0.542
102.5	9.26	2.28	1.370	0.517
112.5	9.72	2.45	1.390	0.578
122.5	10.19	2.54	1.340	0.563
132.5	10.65	2.65	1.510	0.535
142.5	11.12	2.70	1.340	0.534
152.5	11.54	2.74	1.200	0.572
172.5	12.39	3.60	1.290	0.578

TABLE 1. (continued)

Depth in Core cm	Age ka	Calcite wt %	Organic Carbon wt %	Dry Bulk Density* gm/cm2/kyr
192.5	13.24	4.85	1.340	0.584
212.5	14.10	6.49	1.140	0.586
234.5	15.03	7.29	1.070	0.621
250.5	15.71	6.67	0.860	0.670
272.5	16.65	8.61	0.850	0.653
292.5	17.50	7.57	0.820	0.646
312.5	18.35	6.71	0.830	0.611
332.5	19.20	3.16	0.760	0.640
352.5	20.05	4.09	0.830	0.662
372.5	20.90	5.39	0.870	0.612
392.5	21.75	2.79	0.760	0.654

*Based on regression between rho-dry and water content at each site.

They are so bioturbated as to be barely recognizable as layers, and magnetic susceptibility measurements show that they have no fining-upward sequence above them.

We dated three intervals in the piston core by AMS ^{14}C dating on planktonic foraminifera (Table 2). We constructed the chronostratigraphy on these three dates and upon two inflections in the $CaCO_3$ curve, at 8.3 Ka and 11.3 Ka correlated to the Midway core (Figure 5). Other conventional ^{14}C dating in the general vicinity of Gorda Ridge show that these $CaCO_3$ inflections have chronostratigraphic significance [Karlin and Lyle, 1986; Karlin et al., 1992].

The simplest fit of the age data requires a reduction in sedimentation rate at 11.2 Ka, from 23.5 cm/kyr in the older sediments to 21.5 cm/kyr in the younger ones. Assuming that the Holocene sedimentation rate was constant, 100 cm is missing from the top of the piston core. Coring artifacts in either the piston core or its trigger weight gravity core made it difficult to splice the two depth records; the sedimentary section in the trigger core is compressed with respect to the piston core. For example, the interval between the two $CaCO_3$ inflection points is 70 cm in the trigger core and 100 cm in the piston core. The trigger core also has dry bulk densities that are 10-20% higher than in the piston core. We constructed a sedimentation rate profile for the trigger core, assuming no core top loss, with a rate of 20 cm/kyr between 14.3 and 11.8 Ka, 16 cm/ kyr between 11.8 and 4.9 Ka, and a rate of 13cm/kyr between 4.9 Ka and the present.

The Nearshore oxygen isotope profile and the Midway profile are compared in Figure 6 to the high-resolution stack of

TABLE 2. Radiocarbon Data

Core W8709A-	Carbon Type	∂13C § o/oo	Top Depth cm	Bottom Depth cm	Radiocarbon Age ka	Calendar Age ◊ ka
8tc*	C-org	-24.36	0	1	7.47	3.67
8tc	C-org	-22.91	27	28	6.94	3.05
8tc	C-org	-23.26	77	78	10.44	7.14
8tc	C-org	-22.97	125	126	15.30	12.82
8tc	planktonic forams	0.27	120	130	11.56	12.75
8tc	planktonic forams	-0.04	150	160	15.13	16.92
8pc†	planktonic forams	-0.02	160	165	15.04	16.82
8pc†	planktonic forams	-0.22	190	195	17.77	20.01
8pc†	planktonic forams	-0.21	220	225	20.20	22.85
8pc†	planktonic forams	-0.38	251	256	20.44	23.13
13pc	planktonic forams	-0.40	270	275	14.55	16.25
13pc	planktonic forams	-0.37	330	335	17.65	19.87
13pc	planktonic forams	-0.54	390	395	19.10	21.57

* apparently contaminated with plastic coreliner

† depths include the addition of 140 cm, to splice with the trigger core

§ from AMS analysis

◊ Correction from Zahn et al. [1991]

TABLE 3. Stable Isotope Data

Depth in Core cm	∂O-18 (uvi) o/oo	∂C-13 (uvi +0.9) o/oo
	Gyre, W8709A-1BC	
6	3.45	-0.29
11	3.69	-0.48
16	4.23	-0.43
21	4.52	-0.46
26	4.55	-0.41
31	4.43	-0.35
41	4.57	-0.35
	Midway, W8709A-8TC	
3.5	3.45	
39.5	3.04	0.045
59.5	3.19	-0.176
79.5	3.42	-0.11
102.5	3.78	-0.223
120.5	4.11	-0.092
140.5	4.69	-0.171
160.5	4.98	-0.422
180.5	5.14	-0.313
	Midway, W8709A-8PC*	
152.5	4.87	-0.40
162.5	5.09	-0.39
172.5	5.18	-0.52
182.5	5.22	-0.49
192.5	5.18	-0.42
202.5	5.11	-0.39
212.5	5.08	-0.45
222.5	4.99	-0.39
232.5	5.03	-0.46
242.5	5.04	-0.48
253.5	4.97	-0.31
263.5	4.97	-0.34
272.5	4.92	-0.30
282.5	5.13	-0.32
302.5	4.87	-0.35
312.5	4.45	-0.45
340	4.87	-0.48
350	4.89	-0.26
360	4.87	-0.27
370	4.85	-0.13
380	4.83	-0.37
390	4.78	-0.15
400	4.76	-0.35
410	4.85	-0.29
420	4.79	-0.35
430	4.75	-0.35
440	4.81	-0.18
460	4.63	-0.10
480	4.55	-0.26
500	4.62	-0.13

TABLE 3. (continued)

Depth in Core cm	∂O-18 (uvi) o/oo	∂C-13 (uvi +0.9) o/oo
520	4.68	-0.10
540	4.52	-0.18
560	4.50	-0.32
580	4.50	-0.19
600	4.60	-0.23
620	4.45	-0.33
640	4.55	-0.38
660	4.64	-0.36
680	4.61	-0.49
700	4.71	-0.48
740	4.55	-0.58
760	4.41	-0.26
780	4.35	-0.51
800	4.20	-0.24
820	4.02	-0.25
860	3.91	-0.13
900	4.24	-0.33
920	4.26	-0.41
940	3.97	0.10
980	3.93	0.28
1013	3.89	0.06
	Nearshore, W8709A-13PC	
40	3.51	-0.05
60	3.66	-0.20
80	3.62	-0.15
100	4.01	
120	3.81	-0.20
140	4.12	-0.03
170	4.33	-0.32
190	4.57	-0.25
210	4.58	-0.08
230	4.84	-0.28
248	4.98	-0.22
270	5.14	-0.27
290	5.08	-0.39
310	5.01	-0.41
330	4.97	-0.36
350	4.83	-0.38
370	4.87	-0.36
390	4.86	-0.30
420	4.78	-0.35
440	4.78	-0.31

*depth in core + 140 cm overpenetration

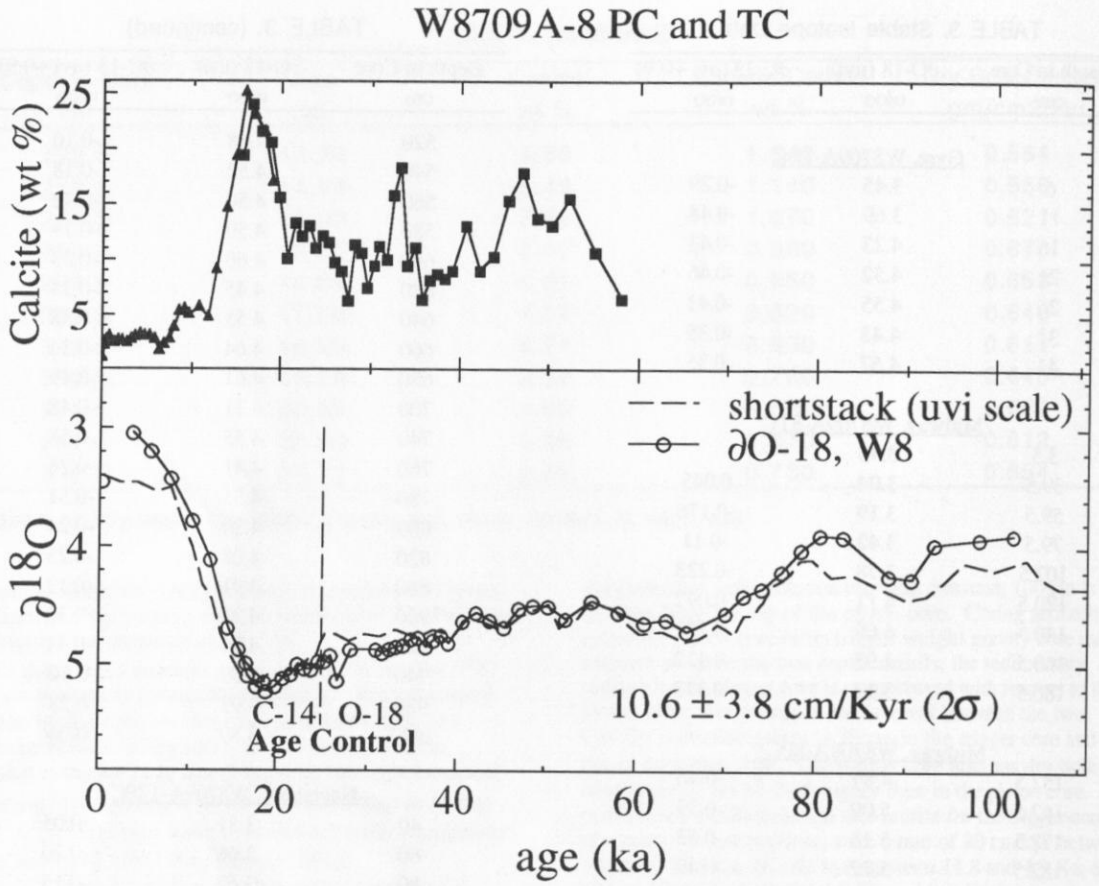

Fig. 4. Comparison of W8709A-8TC & PC oxygen isotope profile from Midway to he high resolution oxygen isotope stack of Martinson et al., [1987]. Note also the $CaCO_3$ profile, which will also be used for stratigraphy at Nearshore.

Martinson et al , [1987]. Ironically, the section constrained only by the $CaCO_3$ stratigraphy fits the oxygen isotope stack better than the section constrained by radiocarbon dates. Since W8709A-8 and W8709A-13 both use ^{14}C ages corrected by the same assumptions, the 2000-year age offset between the Nearshore and Midway oxygen isotope maximum may reflect some residual errors in the time scale.

PATTERNS OF CARBON BURIAL DURING THE HOLOCENE

C_{org} preservation in the Multitracers Transect, estimated by comparing C_{org} MAR in the sediments to the C_{org} rain rate through the water column, is not constant. A strong gradient exists away from the continent, with good preservation near the coast and poor preservation offshore. Calcium carbonate preservation, on the other hand, exhibits no such pattern. The C_{org} preservation gradient has not yet been duplicated by modeling studies [Emerson, 1985; Rabouille and Gaillard, 1991] and is without proper theoretical understanding. C_{org} preservation along the Multitracers Transect is similar to other hemipelagic regions, where no significant correlation between C_{org} burial and bottomwater oxygen, extent of oxic C_{org} degradation, or sediment mixing has been found [Henrichs and Reeburgh, 1987; Jahnke, 1990, Betts and Holland, 1991]. These studies did find a good correlation between C_{org} burial and either C_{org} rain rate or bulk sedimentation rate.

Organic matter: The C_{org} rain rates are derived from 2.5 years of sediment trap data for the Nearshore and Midway mooring sites and 2 years of data at Gyre (Figure 7). The C_{org} rain rate has high variability at all of the Multitracers moorings. The Nearshore rain rates, for example, vary seasonally from almost 700 to less than 200 μg $C/cm^2/yr$. The interannual variability is also high. The highest rain rate was in April 1988, while April 1989 had merely an average flux. High interannual variability was also observed by Thomas and Strub [1989] in Coastal Zone Color Scanner chlorophyll data for 1983-1986 and may be typical of the area. At Midway the seasonal variability is also high, but the interannual variability may be somewhat lower. High spring and summer C_{org} rain rate events persist in the record. At Gyre, we observe a much more regular time series. The highest C_{org} rain rate is typically found in the spring, with a weak fall maximum.

Despite the high seasonal variability we have observed, the average annual C_{org} rain rate at each site is relatively constant (Table 4). The Nearshore rain rate averages 430

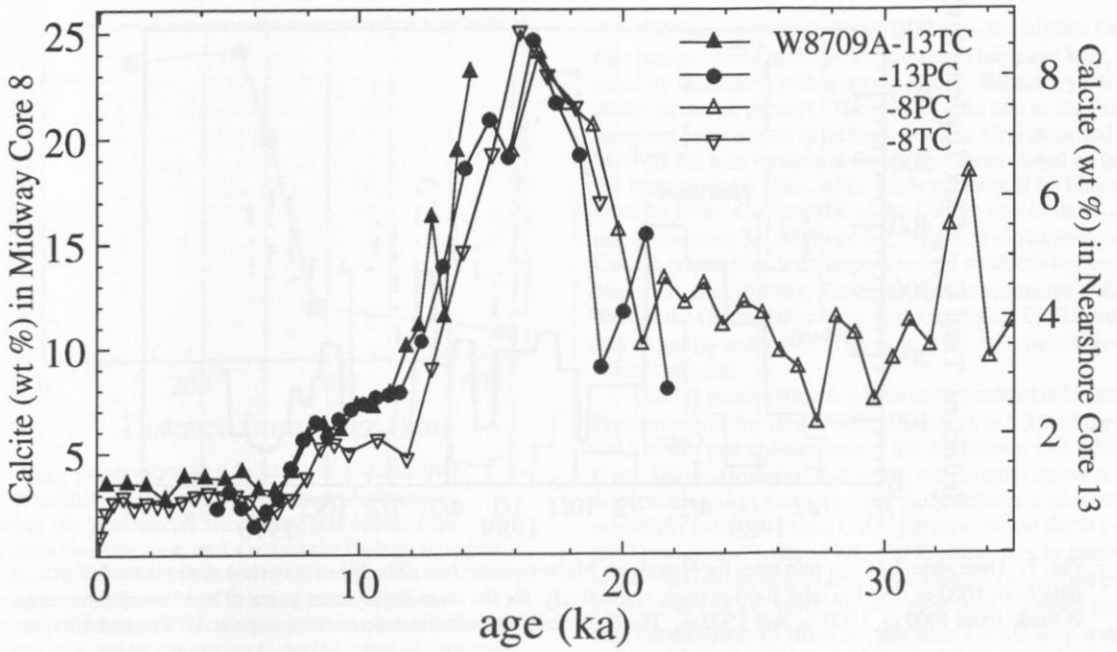

Fig. 5. Comparison of the Midway core W8709A-8 CaCO3 curve to that of the Nearshore core W8709A-13, using the final time scales in each core. Note the CaCO3 peak at 16 Ka and the plateau between 11.5 and 8 Ka.

$\mu gC/cm^2/yr$ over the 2.5 years of the record and varies by only 17% from year 1 to year 2. Midway averages 184 $\mu gC/cm^2/yr$ and varies by 28%, and Gyre averages 98 $\mu gC/cm^2/yr$ and varies by 16%. The gradient in average C_{org} rain rate from Nearshore to Gyre also appears in the individual collection cup data from each sediment trap mooring (Figure 7). Nearshore consistently has the highest seasonal C_{org} rain rate, followed by Midway and then by Gyre.

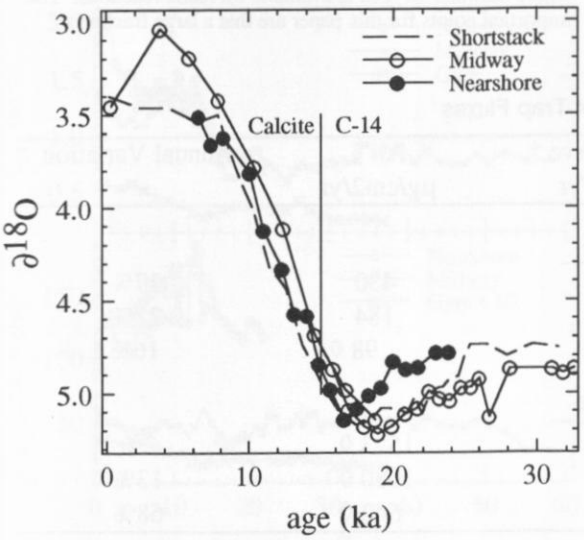

Fig. 6. A comparison of the Nearshore (13PC) and Midway (8PC & TC) oxygen isotope curves to the Martinson et al., [1987] stack. Note that the upper part of W13 has age control by correlation of $CaCO_3$ profiles, while the lower part is controlled by radiocarbon dating.

This pattern has important biological implications for particulate C_{org} production along the Multitracers Transect. The modern C_{org} production gradient cannot be ascribed to the frequency that seasonally upwelled coastal waters are advected to each site. If this were the case, the differences in rain rate between sites would be restricted to the summer/fall upwelling period. High C_{org} rain rates also occurred in winter, when winds recorded at the nearby North Bend (Oregon) airport were unfavorable for upwelling. Second, simple physical limitations on phytoplankton growth rates, such as the amount of insolation on the sea surface, cannot be the primary cause of variation since they would not produce the onshore-offshore gradient. Third, the gradient cannot be produced by high deposition of terrestrial C_{org} near the coast: analyses of the lipid fraction in the surface sediments (discussed later) show that each site's sediments contain about the same proportion of terrestrial C_{org}. If the gradient in C_{org} rain rate is due to nutrient availability in the euphotic zone, there must be a mechanism that supplies Nearshore waters with more nutrients the year round. While a further discussion of this problem is beyond the scope of this paper, we emphasize that primary productivity and what controls productivity changes are poorly understood in the modern oceans. The lack of understanding of modern processes severely limits the ability by paleoceanographers to interpret paleoproductivity records.

The onshore-offshore gradient in C_{org} rain rate appears also as a gradient in C_{org} MAR but is intensified by preservation effects as a function of distance from shore (Figure 8). The data are from the Multitracers moorings and from two other long-term moorings in the northeast Pacific. Preservation has been calculated (1) by comparing the C_{org} rain rate from the 1000-m sediment traps to the sedimentary C_{org} MAR, and (2) by assuming that Al acts as a conservative

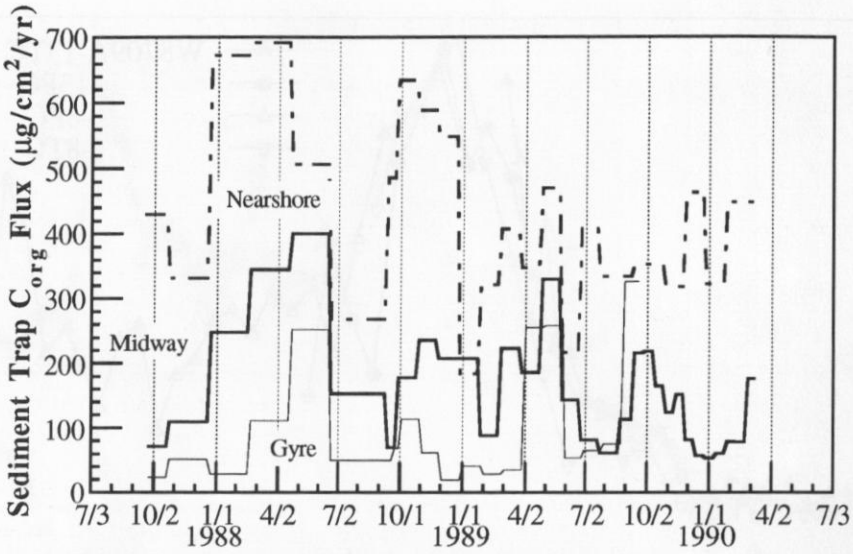

Fig. 7. Time series of C_{org} rain rates for Nearshore, Midway, and Gyre. The Nearshore time series is made from data from 1000-m, 1500-m, and 1000-m traps, respectively, for the three deployment years. The Midway time series is made from 1000 m, 1500 m, and 1500 m. The Gyre time series is constructed from traps at 1750 m and 1500 m.

element in both the traps and the sediments and comparing C_{org}: Al in both [Dymond and Lyle, 1992]. The two methods give similar results. Between the coast and approximately 300 km from shore C_{org} preservation is very high, greater than 20% of the entire flux through the water column. A recent model of organic carbon preservation predicts a similar level of preservation at Nearshore [Rabouille and Guillard, 1991] but underestimates the observed C_{org} preservation at Midway by about a factor of 4. Nevertheless, the preservation rates we observe are not unusual but are similar to C_{org} preservation in other sediments with similar sedimentation rates [Müller and Suess, 1979; Henrichs and Reeburgh, 1987; Betts and Holland, 1991].

Between 300 km to 400 km offshore, preservation sharply drops to about 5% of the C_{org} rain rate. Although this rate is low compared to sediments nearer the coast, C_{org} preservation in pelagic sediments is typically only 1-3% of the total C_{org} rain [Dymond and Lyle, 1985]. Why preservation drops so dramatically and why there is a correlation between preservation and sedimentation rate is unknown. Redox conditions within the sediments may play a part (Figure 3) but the slow sedimentation rates west of the Midway mooring also imply that organic matter remains longer near the benthic interface where the majority of benthic organisms reside, and where seawater oxygen is available for redox reactions. The important points for this paper are that a large fraction of

TABLE 4. Sediment Trap Fluxes

Site	1st Year Ave * µg/cm2/yr	2nd Year Ave † µg/cm2/yr	All § µg/cm2/yr	Annual Variation
		C-org		
Nearshore	486	412	430	17%
Midway	229	178	184	28%
Gyre	90	106	98 ◊	16%
		Calcite		
Nearshore	1536	1510	1523 ◊	2%
Midway	1012	1147	1080 ◊	13%
Gyre	425	859	642 ◊	68%

* October 1987 to October 1988.
† October 1988 to October 1989.
§ October 1987 to March 1990.
◊ October 1987 to October 1989.

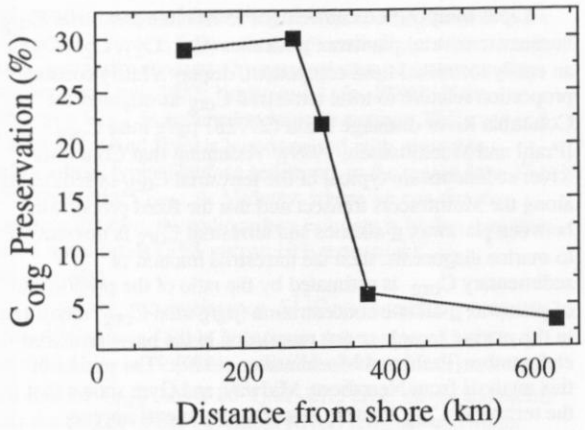

Fig. 8. C_{org} preservation as a function of distance from shore, at northeast Pacific sediment trap deployments (including the Multitracers sites, a site just south of the Mendocino Fracture zone, and a site on the Endeavour segment of the Juan de Fuca Ridge), based upon comparison of 1000-m flux caught in sediment traps to burial rates. Similar preservation rates can be calculated assuming that Al behaves conservatively and by comparing C-org/Al ratios in traps and surface sediments [Dymond and Lyle, 1992].

organic matter has been preserved at both Nearshore and Midway and that sedimentation rate changes since the last glacial maximum are too small to affect C_{org} preservation significantly. Such high C_{org} preservation means that the C_{org} burial is a good reflection of C_{org} rain. Provided that the terrestrial C_{org} component has remained relatively constant, C_{org} burial should reflect paleoproductivity.

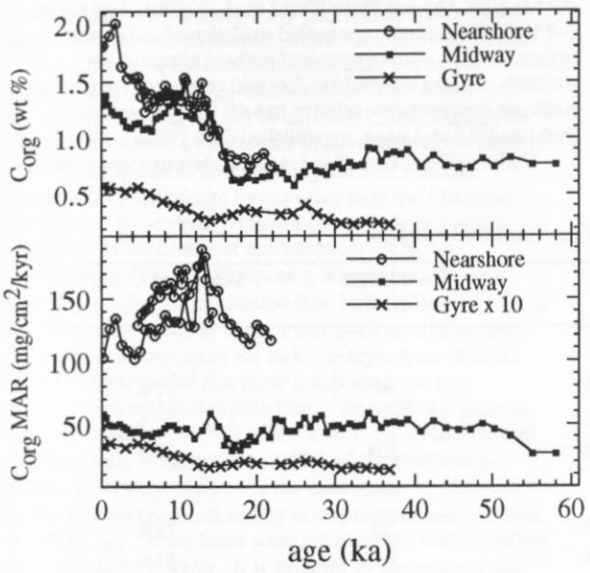

Fig. 9. Profiles of C_{org} content (weight %) and C_{org} MARs for the Multitracers cores. Although the C_{org} percentage has increased dramatically in Holocene sediments, the MARs do not change in the same manner.

Calcium carbonate: At all three sites, the highest $CaCO_3$ rain rates occurred in the period between March and May, possibly associated with a spring bloom. Subsidiary fall peaks were also present. The $CaCO_3$ rain rate in the two sampling years seems to be fairly stable at Nearshore and Midway but was variable at Gyre. Nearshore varied by only 2% between the 2 years, while Midway changed by 13% and Gyre by 68%. Comparison of the $CaCO_3$ rain to the C_{org} rain (Nearshore 3.5, Midway 5.9, Gyre 6.5) shows increased $CaCO_3$ production, with respect to total productivity, between Nearshore and Midway. Similarly, surface sediments to the west of the Gorda Ridge have distinctly higher $CaCO_3$/opal ratios than do sediments to the east of the axis, based upon smear slide data.

$CaCO_3$ preservation has little or no gradient offshore. Preservation at the three Multitracers sites is 5.3% of the $CaCO_3$ rain rate at Nearshore, 7.8% at Midway, and 3.6% at Gyre. For the Holocene sediments, preservation shows no depth relationship, because all of the Multitracers sites are essentially below the local $CaCO_3$ compensation depth (~2400 m) [Dymond and Lyle, 1992]. $CaCO_3$ may only be preserved below 2400 m because pore water alkalinity (supported by Pleistocene $CaCO_3$ burial, as described later), is much higher than the alkalinity of Holocene northeast Pacific deep waters. Provided that part of the Holocene $CaCO_3$ rain can be buried by bioturbation, some is preserved in the sediments.

CARBON BURIAL SINCE THE LAST GLACIAL MAXIMUM

Organic matter: At each of the Multitracers sites the sedimentary C_{org} content has doubled since 15 Ka (Figure 9). This large increase is mostly caused, however, by lower aluminosilicate deposition in the Holocene rather than by increases in total C_{org} burial. At Gyre, C_{org} MARs have almost doubled since the last glacial maximum. At Midway, they are about 40% higher in the Holocene than 18 Ka. Prior to 24 Ka, however, C_{org} MARs were similar to Holocene rates. At Nearshore, 18 Ka and the present have about the same C_{org} MAR. During deglaciation, however, C_{org} MARs were almost 50% higher than either Holocene or Pleistocene deposition.

C_{org} MAR transects (Figure10) illustrate that the net burial across the northern California Current was lower at the last glacial maximum. Assuming exponential decrease of C_{org} MARs away from the continent for both time slices, the integrated C_{org} deposition between Nearshore and Gyre was 20% lower at 18 Ka than at 1 Ka. Thus, despite the spectacular change in C_{org} content in the Multitracers cores, the change in total C_{org} burial before and after the deglaciation was minor and primarily occurred away from shore. If the terrestrial fraction of the total C_{org} has been relatively constant, there was only a minor drop in marine productivity.

The transport and burial of terrestrial C_{org} along the Multitracers Transect has probably varied since 18 Ka. Nearshore had twice the burial rate of terrestrial aluminosilicate detritus at 18 Ka than for the Holocene (Figure10) while Midway had 25% higher and Gyre had about the same aluminosilicate MAR. High glacial aluminosilicate MARs may indicate high terrestrial C_{org} MARs.

Terrestrial versus marine C_{org} burial: We used the lipid geochemistry of the organic fraction to make an estimate of terrestrial C_{org} in Multitracers sediments and checked our

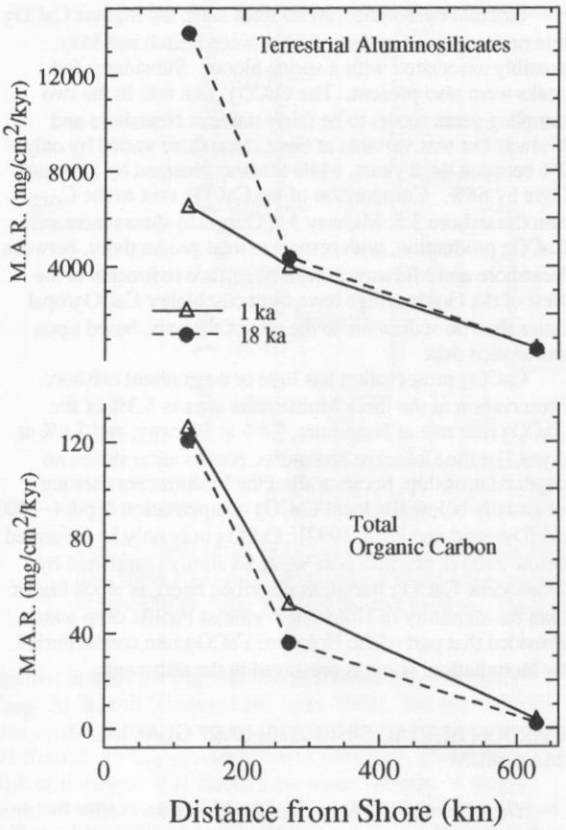

Fig. 10. Time slices at 1 Ka and 18 Ka to illustrate how terrestrial sediment (bulk - CaCO3) and C_{org} MAR gradients differed between the last glacial maximum and the present. The Nearshore site had almost twice as much terrestrial detritus being deposited at 18 Ka.

estimates by means of radiocarbon dates and by reconnaissance stable carbon isotope measurements on bulk sedimentary C_{org}. We do not yet have complete time series but have sufficient data to compare glacial maximum sediments to modern ones.

Lipid composition can be used to estimate terrestrial C_{org} because terrestrial plantwax n-alkanes (C_{25}, C_{27}, C_{29}, C_{31}), an easily identified lipid component, display a fairly constant proportion relative to total terrestrial C_{org} throughout the Columbia River drainage basin (277±87 µg/g total C_{org}) [Prahl and Muehlhausen, 1989]. Assuming that Columbia River sediments are typical of the terrestrial C_{org} in sediments along the Multitracers transect and that the fixed proportion between plantwax n-alkanes and terrestrial C_{org} is insensitive to marine diagenesis, then the terrestrial fraction of sedimentary C_{org} is estimated by the ratio of the proportion of plantwax n-alkane concentration (µg/g total C_{org}) measured in the marine sample to the proportion in the pure terrestrial endmember [Prahl and Muehlhausen, 1989]. The results of this analysis from Nearshore, Midway, and Gyre shows that the terrestrial C_{org} fraction in surface sediments appears relatively constant, averaging 20±3% (Table 5). For both Nearshore and Midway, the percentage of terrestrial C_{org} is 2-3 times higher in the glacial sediment intervals.

The carbon maximum (C_{max}) for the plantwax n-alkane series preserved in sediments along the Multitracers transect is C_{29}, regardless of sampling location or time. This observation implies that all samples share a common terrestrial source for the C_{org} [Prahl et al., 1989a]. One can speculate that the offshore increase in the hydrocarbon estimate of terrestrial C_{org} reflects the more refractory nature of terrestrial versus marine C_{org} in early diagenesis and does not indicate measurement uncertainty. Our sediment trap/sediment comparisons suggest that there is an offshore decrease in sedimentary C_{org} preservation. If plantwax n-alkanes are more refractory than bulk sedimentary C_{org}, enrichment of these biomarkers relative to total C_{org} should occur in more degraded fractions. Notably, differential decomposition rates between plantwax n-alkanes and total C_{org} (a blend of terrestrial and marine C_{org}) have been shown in a recent study of postdepositional oxidation effects on a turbidite layer from the Madeira Abyssal Plain [Prahl et al., 1989b]. Long-term (~8 kyr), diffusionally controlled oxidation of sedimentary organic matter, with oxygen and perhaps nitrate as the oxidants, led to a threefold to fourfold enrichment in plantwax n-alkane concentration relative to total C_{org} content (F.G. Prahl and G.J. deLange, unpublished data, 1991).

Radiocarbon analyses and stable carbon isotopes provide

TABLE 5. Lipid Estimate of the Terrestrial Fraction

Core Name	Depth in Core cm	Age ka	Σn-alkanes *	Terrestrial C-org**
Nearshore				
W8709A-9BC	0-1	0.03	46	17%
W8709A-13PC	8- 10	4.9	63	23%
W8709A-13PC	322-324	18.6	108	39%
Midway				
W8709A-6BC	0-1	0.05	52	19%
W8709A-8TC	170-174	17.8	141	51%
Gyre				
W8709A-BC1	0-1	0.4	64	23%

* ΣC25,C27,C29,C31 terrestrial plant wax n-alkanes, micrograms per gram total C-org.

† estimate based upon 277±87 µg/gC-org n-alkanes in terrestrial organic matter [Prahl and Muehlhausen, 1989].

independent ways of estimating terrestrial C_{org} content of the sediments. Table 6 lists surface radiocarbon ages from nearby cores, primarily estimated by extrapolation of downcore data [Karlin and Levi, 1985; Karlin and Lyle, 1986]. If the terrestrial C_{org} is assumed to have an average 20 Ka age and if a 10 cm mixed layer is homogenized with respect to radiocarbon, typical surface sediments in the region have 15 to 35% terrestrial C_{org}. At Midway, where we can directly compare the two, the radiocarbon estimate is higher than that based upon lipids (35% versus 19% terrestrial C_{org} respectively).

Similarly, reconnaissance $\delta^{13}C$ measurements from the AMS ^{14}C dating (Table 2) indicate that roughly 35-40% of the total C_{org} in Holocene sediments is terrestrial, assuming that marine C_{org} has a $\delta^{13}C$ of -21.5 o/oo (from sediments near the mouth of the Columbia River) [Hedges and Mann, 1979] and terrestrial C_{org} is -25.5 o/oo (Columbia River terrestrial C_{org}) [Hedges et al., 1984]. An independent estimate of the $\delta^{13}C$ of Holocene marine C_{org} based upon equilibrium with modern preanthropogenic atmospheric pCO_2 and measured sea surface temperatures (-21.4 o/oo [Rau et al., 1991a, 1991b]) yields virtually the same fractionation as measured by Hedges and Mann [1979]. If equilibrium surface water pCO2 changed in accordance with the atmospheric profile of Barnola et al. [1987] and sea surface temperatures in accordance with our own unpublished profiles, the marine C_{org} end member should have been less depleted in ^{13}C in the latest Pleistocene and earliest Holocene. The sediments of this age probably contain more terrestrial C_{org} than the present, even though the measured $\delta^{13}C$ in the interval is virtually the same as younger sediments.

The reason why terrestrial C_{org} estimates determined by hydrocarbon (lipid) analysis are lower than those based upon radiocarbon and stable carbon isotopes is not yet known. While part of the discrepancy may be due to inaccuracies associated with the radiocarbon and stable carbon isotope models, it may also reflect poorly understood systematics of terrestrial biomarker production, deposition, and diagenesis.

The Columbia River end member may not be the appropriate terrestrial C_{org} end member at the Multitracer sites. Rivers such as the Eel in northern California may be the dominant source of terrestrial C_{org} to this region [Karlin, 1980]. A comparative study of the plantwax n-alkane geochemistry for drainage basins other than the Columbia River has yet to be done. It is not certain whether some degradation of the plantwax n-alkanes occurs in the Multitracers sediments. Plantwax n-alkanes appear more resistent to oxidative degradation than bulk sedimentary C_{org}. Nonetheless, the analysis of plantwax n-alkanes in oxidized and unoxidized portions of the turbidite layer from Madeira Abyssal Plain revealed that these compounds are not impervious to oxidative destruction. The oxidation process which destroyed about 90% of the total C_{org} in the turbidite layer apparently destroyed about 50% of the plantwax n-alkanes. It is not yet known if the destruction of plantwax n-alkanes occurred proportionately or disproportionately to bulk terrestrial C_{org}. If the latter were the case, the binary mixing model would be in error. It is difficult to speculate at this time whether the model would underestimate or overestimate the terrestrial C_{org} fraction.

The terrestrial C_{org} estimates based on the stable carbon and radiocarbon analyses also may have considerable error attached to them. Note that the $\delta^{13}C$ values measured for

TABLE 6. Radiocarbon Estimates of the Terrestrial Fraction

Core Name	Latitude °N	Longitude °W	Water Depth m	Sedimentation Rate cm/kyr	Surface Age years b.p.	Model % Terrestrial 20 ka age	Model % Terrestrial 10 ka age
W7710A-28 KC	44°50.1	125° 7.5'	1825	121	2020	16	22
W8508A-09 GC	43°01.8'	126°34.7'	3150	6	3500	24	35
L6-85-NC-1 GC	41°07.2'	127°30.2'	3200	15	3200	26	37
L6-85-NC-8 GC	40°44.5'	127°31.3'	3200	13	3700	31	43
W8709A-8, Midway	42°15.7'	127°40.7'	3111	10	4300	36	50

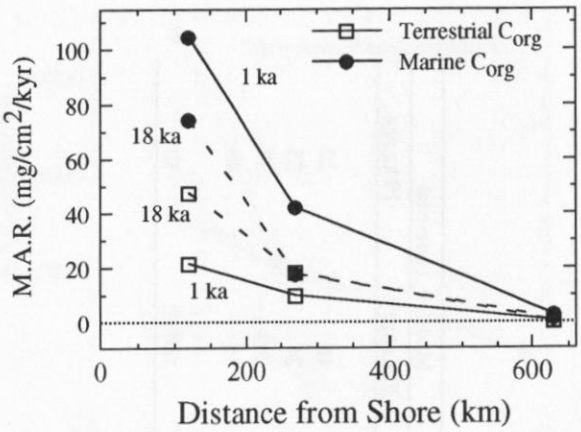

Fig. 11. Marine and terrestrial C_{org} MARs along the Multitracers Transect, at 1 Ka and about 18 Ka. The terrestrial C_{org} fraction was estimated using plant wax *n*-alkanes (see text). Note how the marine C_{org} MARs are much lower at 18 Ka.

total C_{org} in the individual sediments by the AMS technique have an intrinsic uncertainty of about 1 o/oo. Similarly, the large corrections in the radiocarbon ages can introduce significant errors in the terrestrial C_{org} estimates, and we have not considered whether there could be young redeposited marine C_{org} in the sediments. Nevertheless, all three methods agree that the terrestrial C_{org} fraction is a large percentage of the total sedimentary C_{org} along the Multitracers Transect.

Pleistocene sediments at the Nearshore and Midway locations have higher plantwax n-alkane contents (μg/g total C_{org}) than do Holocene sediments, and by the interpretation presented above, contain greater contents of terrestrial C_{org} (40-50% terrestrial versus 20% in the Holocene; Table 5). Although the absolute quantity of terrestrial C_{org} is debatable, we conclude with confidence that the marine C_{org} fraction was a much smaller proportion of the total sedimentary C_{org} pool at 18 Ka than it is at present. The terrestrial and marine C_{org} MARs along the Multitracers Transect for time slices at 1 Ka and 18 Ka are plotted in Figure 11, based on the lipid analyses (Table 5). The terrestrial C_{org} fraction at Gyre was assumed to be unchanged from 18 Ka to the present. Note that the marine C_{org} MARs more than double from the last glacial maximum to the present even though the total C_{org} MARs change by only about 20% (Figure 10). Marine C_{org} MARs have thus increased significantly since 18 Ka across the Multitracers Transect, and so, too, must have productivity.

Calcium carbonate: Pleistocene $CaCO_3$ MARs are at least an order of magnitude higher than Holocene $CaCO_3$ MARs along the Multitracers Transect (Figure 12). High $CaCO_3$ burial during glacial climatic intervals is typical of the northeast Pacific [Karlin et al., 1992; Zahn et al., 1992]. The $CaCO_3$ compensation depth in the region rose to about 2400 m during the deglaciation from a depth of about 4500 m water depth [Karlin et al., 1992].

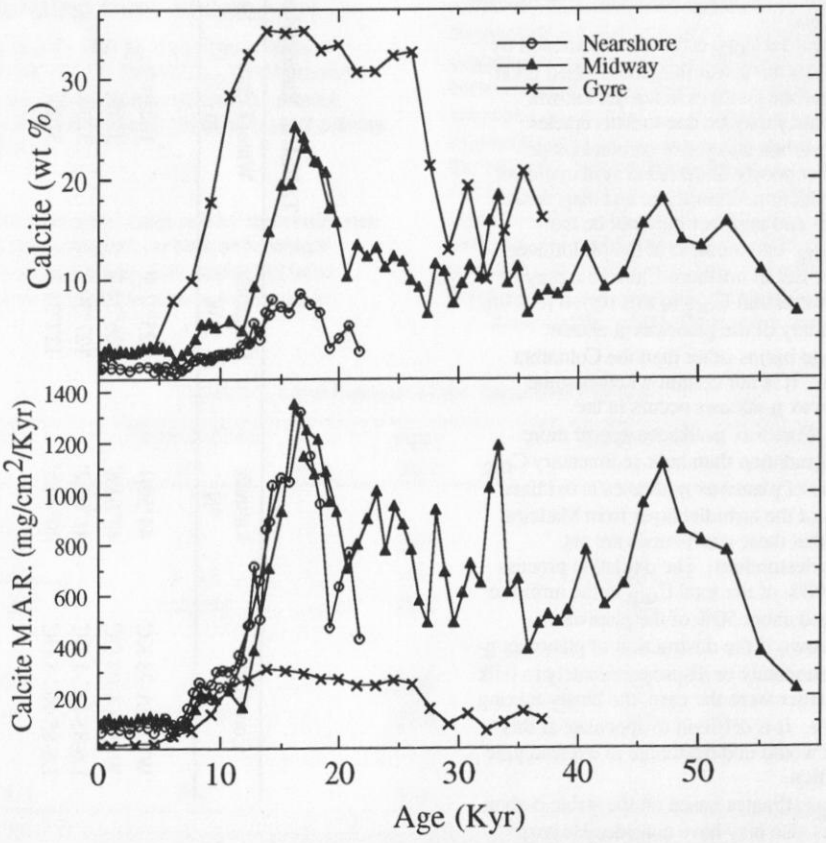

Fig. 12. Sedimentary $CaCO_3$ content and MARs from the Multitracers sites.

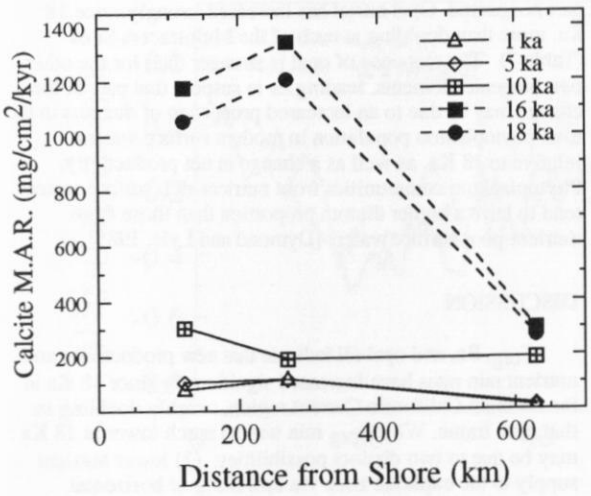

Fig. 13. $CaCO_3$ MAR gradients across the Multitracers Transect for selected time slices since the last glacial maximum. The glacial $CaCO_3$ MARs are about the same as today's $CaCO_3$ rain rate caught in the sediment traps.

Sedimentary $CaCO_3$ profiles along the Multitracers Transect have distinct steps, probably marking major changes in northeast Pacific deepwater properties. The pattern of $CaCO_3$ burial is essentially the same at Nearshore and Midway and is different at Gyre only because of poor resolution induced by the slow sedimentation rate. $CaCO_3$ burial is high during oxygen isotope stage 2 and reaches a peak at about 16 Ka, after the oxygen isotope-marked glacial maximum. After peak $CaCO_3$ deposition, both $CaCO_3$ MARs and sedimentary $CaCO_3$ contents dropped to an intermediate plateau, between 11.5 Ka to 7.5 Ka. After 7.5 Ka they both dropped further to modern values. Figure 13 shows how the $CaCO_3$ MAR changed across the transect through time. The Pleistocene $CaCO_3$ MARs, marked by dashed lines, are high but decrease seaward. Pleistocene $CaCO_3$ MARs at Nearshore and Midway are about the same as Pleistocene MARs in equatorial Pacific sediments [Lyle et al., 1988] (data from Farrell and Prell) [1989].

Offshore, at Gyre, $CaCO_3$ MARs are much lower than they are nearer the coast throughout the sedimentary record (Figure 13). Low $CaCO_3$ MARs at Gyre may be a result partly of the water depth (3600 m versus 2800 m for the other two sites) but are probably also due to a gradient in $CaCO_3$ production offshore. Today, there is about a factor of 2 difference in $CaCO_3$ rain rates between Midway and Gyre (Table 4). A similar gradient should have existed during the Pleistocene, since there is a good correlation between total C_{org} rain and $CaCO_3$ rain in sediment traps [Lyle et al., 1988] (unpublished Multitracers data). $CaCO_3$ MAR most probably has always decreased offshore, even without depth-induced dissolution. For the Pleistocene interval, however, the $CaCO_3$ MAR is a factor of 4 less at Gyre than at Midway and indicates that $CaCO_3$ dissolution occurred between 2800 and 3600 m then.

The Pleistocene $CaCO_3$ MARs at Nearshore and Midway are nearly equal to today's $CaCO_3$ rain. Since $CaCO_3$ probably did dissolve from the Pleistocene sediments, $CaCO_3$ production in the surface waters was probably somewhat higher at 18 Ka than today. It is impossible now to estimate whether the change in $CaCO_3$ production was small or large. To do so will require either better modeling of the carbon cycle or will require the development of a proxy indicator for $CaCO_3$ production.

PALEOPRODUCTIVITY AT 18 Ka

Table 7 shows the change in estimated marine C_{org} rain rate (based upon the marine C_{org} MAR) to other indices of paleoproductivity. We chose not to try to estimate primary productivity per se, because modern measurements are highly variable along the transect and do not yet form a good calibration set (P. Wheeler, personal communication, 1991). Moreover, new productivity (particulate C_{org} flux from the euphotic zone) [Eppley and Peterson, 1979] is the key information needed to understand biogeochemical cycles, not net primary productivity. A primary productivity estimate is useful mostly for studies of the dynamics of biological communities.

Marine C_{org} rain rate: For the estimate we assumed that C_{org} preservation is the same at 18 Ka as today and that the C_{org} fraction which degrades within the topmost sediments is marine in origin. Terrestrial biomarker contents in the sediment traps are low and must be diluted by a larger fraction of marine material than surface sediments (F. Prahl, unpublished data, 1991). Thus, most of the material that degrades at the benthic interface must be labile marine organic matter. The assumption of constant C_{org} preservation since 18 Ka may introduce some errors, but because sedimentation rates did not change strongly and because C_{org} preservation is high and to the first order a function of sedimentation rate [Henrichs and Reeburgh, 1987] there probably was not a large change. We observe a consistent pattern in which the estimated 18 Ka marine C_{org} rain rates along the transect are roughly 40 to 70% of modern rates.

Ba: Ba is one of the few elements associated with biogenic detritus that is well-preserved in most marine sediments [Goldberg and Arrhenius, 1958; Church, 1970; Dymond, 1981; Dymond et al., 1992]. Barite is precipitated in microenvironments by decomposition of particulate organic matter [Bishop, 1988] and thus mimics C_{org}. Like C_{org}, a large fraction of the sedimentary Ba in hemipelagic sediments is bound in a terrigenous fraction, in this case aluminosilicates [Dymond et al.,1992]. Ba MAR profiles near continents must therefore be corrected for the terrigenous Ba fraction in order to discern the paleoproductivity signal. At Nearshore the terrigenous correction is so large that a minor change of the assumed terrigenous Ba:Al can completely change the shape of the Ba MAR profile; thus corrected biogenic Ba MAR profiles are suspect. At Midway and Gyre, however, the terrigenous correction is relatively minor. Our estimates of biogenic Ba flux show that modern fluxes of biogenic Ba are higher than at 18 Ka by roughly a third and a quarter, respectively, for Midway and Gyre (Table 7). The change in biogenic Ba flux indicates similar but somewhat smaller productivity changes since 18 Ka than estimated C_{org} rain.

Opal: Opal MARs are another index of paleoproductivity, since opal is in large part produced by marine diatoms [Lyle et al., 1988]. In the Multitracers transect, Pliocene freshwater diatoms contribute a small percentage to the opal contents of glacial sediments [Sancetta et al., 1992] and opal phytoliths from terrestrial plants are probably also a small fraction of the total sedimentary opal. Nevertheless, these terrestrial contributions can for the most

TABLE 7. Changes in Biogenic Fluxes along the Multitracers Transect

Core Name	Depth in Core cm	Age ka	Marine C-org MAR mg/cm2/kyr	Fraction of Modern	Estimated Marine C-org Rain Rate (1000 m) µg/cm2/yr	Fraction of Modern	Biogenic Ba MAR* mg/cm2/kyr	Fraction of Modern	Biogenic Opal MAR mg/cm2/kyr	Fraction of Modern
Nearshore										
W8709A-9BC	0-1	0.03	105	100%	409	100%	-	-	1057	100%
W8709A-13PC	8- 10	4.9	106	101%	414	101%	-	-	785	74%
W8709A-13PC	322-324	18.6	71	68%	278	68%	-	-	286.7	27%
Midway										
W8709A-6BC	0-1	0.05	42	100%	174	100%	9.1	100%	193	100%
W8709A-8TC	170-174	17.8	17	41%	71	41%	5.8	64%	74	38%
Gyre										
W8709A-BC1	0-1	0.4	3	100%	97	100%	4.6	100%	25.2	100%
W8709A-BC1	23-25	18.47	2	60%	58	60%	3.4	75%	11.2	44%

*Corrected by: Ba-bio = Ba-tot -Al%(Ba:Al[terr]), where Ba:Al [terr.] = 0.0075 [Dymond et al, 1992]

part be ignored. Opal burial has increased strongly since 18 Ka, more than doubling at each of the Multitracers Sites (Table 7). The response of opal is stronger than for the other two biogenic elements, leading us to suspect that part of the change may be due to an increased proportion of diatoms in the total phytoplanton population in modern surface waters relative to 18 Ka, as well as a change in net productivity. Phytoplankton communities from nutrient-rich surface waters tend to have a higher diatom proportion than those from nutrient-poor surface waters [Dymond and Lyle, 1985].

DISCUSSION

C_{org}, Ba, and opal all indicate that new productivity and nutrient rain rates have increased significantly since 18 Ka in the northern California Current region, roughly doubling in that time frame. Why C_{org} rain was so much lower at 18 Ka may be due to two distinct possibilities: (1) lower nutrient supply to the euphotic zone via upwelling or horizontal advection, or (2) the plankton community was unable to utilize the available nutrients at the last glacial maximum as well as they can today [e.g., Martin, 1990], so new productivity was lower.

In the first case, we have a direct linkage between the flux of dissolved nutrients into the euphotic zone via upwelling or horizontal advection and loss of the nutrients from the euphotic zone to deep waters and the sediments. Under some circumstances, however, phytoplankton cannot utilize all the nutrients available to them in the euphotic zone: 1) a micronutrient may be missing; or 2) physical factors (e.g., light levels or storm mixing) [Riley, 1942] may prevent the phytoplankton from being fully efficient; or 3) high levels of zooplankton grazers may crop the phytoplankton before they can fix all the nutrients. In such a scenario, new productivity could change not because of changes in nutrient supply but because of other important biogeochemical or ecological factors. Such an "inefficient" system exists today in the Alaska Gyre [Miller et al., 1988]. While the region has high primary productivity, it is not sufficient to deplete the surface waters of dissolved nitrates or phosphorus. It is possible that the lower marine C_{org} burial at the last glacial maximum was the result of the same Alaska Gyre community being in place off the Oregon coast. Only the ability of the community to use nutrients would have changed, not the upwelling nutrient fluxes.

The climate change hypothesis: While the above hypothesis cannot yet be eliminated, we prefer to interpret lower glacial productivity off Oregon to be a result of a climatic regime which had a lower flow of nutrients into the surface waters than the one today. Such a reduction could be caused by reduced coastal upwelling, or it could be caused by the replacement of the nutrient-rich subsurface waters found in the north Pacific today with waters significantly poorer in nutrients.

Subsurface nutrients: Late Quaternary $CaCO_3$ and benthic $\delta^{13}C$ records from core sites near the Juan de Fuca Ridge imply that the northeast Pacific carbon system changed dramatically during glacial-interglacial times [Karlin et al., 1992]. The lysocline was nearly 2 km deeper in glacials, as evinced by $CaCO_3$ contents near 80% in 3700 m of water. Since benthic $\delta^{13}C$ records imply higher ΣCO_2 concentrations, the higher $CaCO_3$ ion concentrations required to explain the change in lysocline depth could have been achieved only through higher seawater alkalinity in the

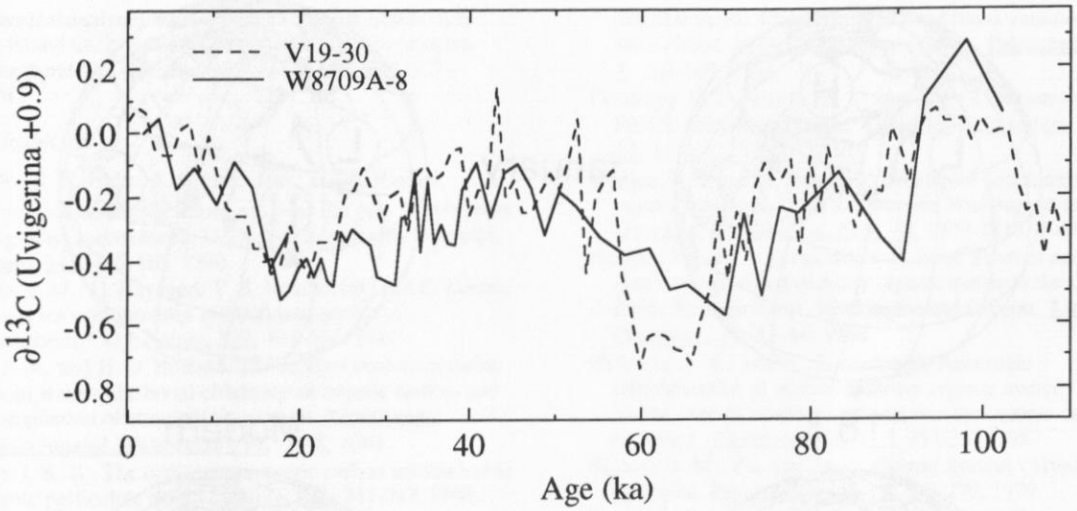

Fig. 14. Comparisons of benthic $\delta^{13}C$ profiles from the Midway site to the eastern equatorial Pacific profile of Shackleton and Pisias [1985]. Both are from Uvigerina species foraminifera, and both have been corrected by +0.9 per mil to reflect bottomwater $\delta^{13}C$. While the two profiles are comparable, the northeast Pacific (Midway) profile is slightly more negative at 18 Ka.

glacials. Glacial-interglacial benthic $\delta^{13}C$ variations at Midway closely resemble those of core V19-30 in the eastern equatorial Pacific (Figure 14) [Shackleton and Pisias, 1985]. The amplitude of 0.55 o/oo is only slightly more than the estimated global "carbon pool" effect of 0.46 o/oo [Curry et al., 1988] that was caused by the growth and destruction of the terrestrial biosphere. The lack of any strong $\delta^{13}C$ shift at Midway different from the global shift implies that North Pacific deep waters carried similar amounts of carbon derived from degraded organic matter at 18 Ka and in the Holocene. Estimates of phosphorus content in deep equatorial Pacific waters [Boyle, 1988] indicate that the nutrient contents there at least did not vary strongly from the last glacial to the present interglacial period. For these reasons we believe that the nutrient contents of north Pacific deep waters were probably high even during the glacials.

Changes in upwelling: If climate is directly a factor in the change in productivity off southern Oregon, it must manifest itself as a change in coastally upwelled water advected outward or as a change in the diffuse upwelling throughout the northeastern Pacific. At the moment, we lack data about changes in ocean circulation associated with the deglaciation because there is no adequate coupled ocean-atmosphere general circulation model. In the absence of oceanographic models, we can still make inferences about coastal upwelling from atmospheric climate "experiments" for the deglaciation (Figure 15) [Kutzbach, 1987; COHMAP members, 1988].

The main contrast of the model glacial atmospheric circulation with the modern is a semipermanent high-pressure region over the North American ice cap. Climatic feedbacks associated with the high pressure over the ice cap resulted in a splitting and movement of the jet stream. They also caused movement of the subtropical north Pacific high pressure regime southward and closer to the North American coast (Figure 15).

During the winter, one branch of the jet stream was diverted north of the ice cap, while the second branch was about 10° south of its modern position -- storms that today come ashore in the Pacific Northwest (~45°N) were diverted along a more southerly route, to southern California (~35°N). Just south of the ice cap, at about the Canada/U.S. border, easterly winds blew offshore in the winter. The existence of this easterly circulation is supported by aeolian transport of Pliocene fresh water diatoms from inland deposits in Idaho and eastern Oregon to sediments in the Multitracers transect and to at least one volcanic crater lake in the region [Sancetta et al., 1992].

The model summer atmospheric circulation was also strongly affected by the ice cap high pressure regime. The northerly (upwelling favorable) winds north of south central California (35°N) were suppressed at 18 Ka by the position of the glacial subtropical high, which at that time occupied a more southerly position nearer to the North American coast. The northwestern UnitedStates was under a ridge between the two high-pressure regimes, and consequently should have had weak and variable summer winds. Today, upwelling along coastal Oregon and California is driven by equatorward winds that roughly parallel the coast [Huyer, 1983]. The winds are seasonally to the south in northern California but are upwelling-favorable all year south of San Francisco. The seasonal cycle of winds and upwelling is a direct result of the seasonal migration of the North Pacific High pressure regime between its southerly position centered at 28°N in February and its northerly position, 38°N, in July [Huyer, 1983].

While it is appealing to link the change in productivity we have observed directly to a simple physical forcing effect (the movement of the North Pacific High and consequent change in winds favorable to upwelling), we must remind the reader that our observations of productivity and C_{org} flux in the modern ocean make us believe that the full explanation of the productivity changes associated with deglaciation will be more complex. In the first two and a half years of sediment trap collection along the transect, we did not observe a correlation between the time of summer upwelling winds and C_{org} rain rate. Instead, we see relatively random periods of high flux at Nearshore, that become more regular and predictable at Gyre (Figure 11). Further work in the modern ocean will help us to refine our paleoceanographic perspective.

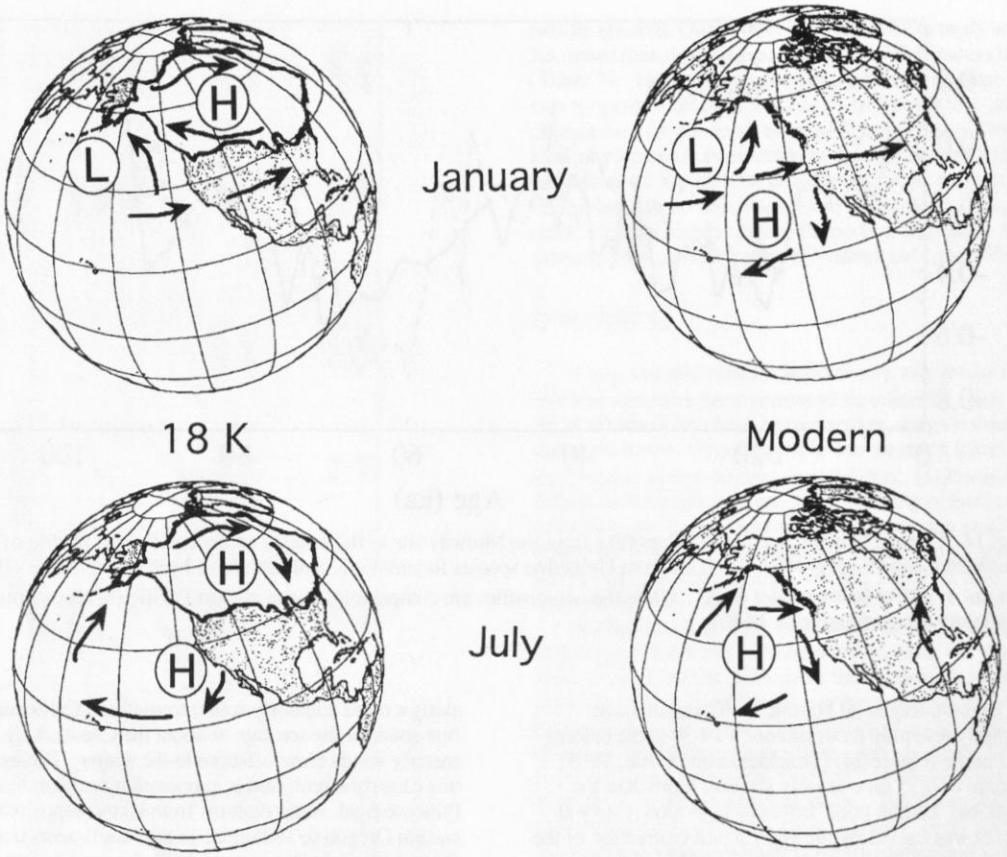

Fig. 15. A comparison of GCM winds for the glacial and modern world [after Kutzbach, 1987; COHMAP members, 1988. The presence of the large ice cap at 18 Ka causes a semipermanent high-pressure field to form over it. The high splits the jet stream in the winter and causes storm tracks to be diverted south of their typical modern position, and in the summer interacts with the north Pacific High to weaken upwelling favorable northerlies winds off Oregon and northern California near 40°N.

CONCLUSIONS

Because of the strong terrestrial imprint on the hemipelagic sediments of the Multitracers Transect and most other nearshore marine sediments, the sedimentary profiles of bulk biogenic components reflect multiple processes. Dilution by terrestrial aluminosilicate detritus can cause major changes in sedimentary biogenic contents. Terrestrial sources can further complicate the sedimentary profiles of C_{org} and Ba. Nevertheless, definition of fluxes in the ocean margins is crucial for understanding biogenic element cycles, since the highest productivity-induced fluxes rim the ocean basins. For example, the C_{org} rain rate at Nearshore is about 4 times higher than sites beneath the equatorial Pacific divergence and in the eastern tropical Pacific [Dymond and Lyle, 1992].

We have documented that conditions along the Multitracers transect at 18 Ka were significantly different than conditions today. The glacial interval was marked by significantly lower productivity, higher $CaCO_3$ burial, and, within about 300 km of shore, much higher terrestrial C_{org} and aluminosilicate MARs. Terrestrial aluminosilicate deposition doubled at Nearshore and was significantly higher at Midway, 270 km from the coast. High terrestrial deposition at 18 Ka also led to significant burial of terrestrial C_{org}, which approached 50% of the total C_{org} fraction at Nearshore and Midway. The marine C_{org}, opal, and Ba profiles (when terrestrial effects are accounted for) indicate that Holocene productivity may be nearly double the glacial productivity. In contrast, highest C_{org} MARs in both the Atlantic and the Pacific equatorial regions occur at the last glacial maximum [Lyle, 1988; Sarnthein et al., 1988].

We have hypothesized that the change in productivity has a direct climatic link, associated with the shift in the mean position of the subtropical North Pacific High. In order to test this hypothesis, however, we need more information about the controls of productivity and marine C_{org} rain rates in the modern California Current, and we need more paleoceanographic records south of the Mendocino Fracture Zone, off California and Mexico. Eventually, with the new data, we can explore the links between climate and productivity and compare climate patterns on the North American continent to paleoceanographic changes offshore.

Acknowledgments. The Multitracers study could not have been done without the high competence of the OSU sediment trap group (J. C. Moser, K. Brooksforce, P. Collier, and a host of temporary employees) and the captain and crew of the R/V Wecoma. Most of the lab analyses reported in this study were conducted by R. Conard, A. Ungerer, and K. Brooksforce. Editing by J. Tivy and A. Olivarez also improved the quality of this paper. The field work and the majority of the data collection was supported by NSF grants OCE-8609366 and OCE-8919956, while the organic

geochemical analyses were supported by NSF grants OCE-8812340 and OCE-9001603. The synthesis of the data has been supported by NSF grants OCE-8911688 and OCE-9000945.

REFERENCES

Bard, E., B. Hamelin, R. G. Fairbanks, and A. Zindler, Calibration of the ^{14}C timescale over the past 30,000 years using mass spectrometric U-Th ages from Barbados corals, Nature, 345, 405-410, 1990.

Barnola, J. M., D. Raynaud, Y. S. Kortkevich, and C. Lorius, Vostok ice core provides 160,000 year record of atmospheric CO_2, Nature, 329, 408-414, 1987.

Betts, J. N., and H. D. Holland The oxygen content of ocean bottom waters, the burial efficiency of organic carbon, and the regulation of atmospheric oxygen. Palaeogeog., Palaeoclimatol., Palaeoecol., 97, 5-18, 1991.

Bishop, J. K. B. The barite-opal-organic carbon association in oceanic particulate matter. Nature, 331, 341-343, 1988.

Boyle, E. A. Cadmium: Chemical tracer of deepwater paleoceanography, Paleoceanography, 3, 471-491, 1988.

Church, T. M. Marine barite. Ph.D. thesis, 100 pp., Univ. of Calif., San Diego, 1970.

COHMAP Members, Climatic changes of the last 18,000 years: Observations and model simulations, Science, 241, 1043-1052, 1988.

Curry, W. B., J. C. Duplessy, L. D. Labeyrie, and N.J. Shackleton , Changes in the distribution of $\delta^{13}C$ of deepwater ΣCO_2 between the last glaciation and the Holocene, Paleoceanography, 3, 317-341, 1988.

Dehlinger, P., R. W. Couch, D. A. McManus, and M. Gemperle, Northeast Pacific structure in The Sea , vol. 4, part 2, edited by A.E. Maxwell, pp. 133-190, John Wiley, 133-189, New York, 1971.

Dymond, J., Geochemistry of Nazca Plate surface sediments: An evaluation of hydrothermal, biogenic, detrital, and hydrogenous sources, Geol. Soc. Am. Mem., 154, 133-175, 1981.

Dymond, J., and M. Lyle, Flux comparisons between sediments and sediment traps in the eastern tropical Pacific: Implications for atmospheric CO2 variations during the Pleistocene, Limnol. Oceanogr., 30, 699-712, 1985.

Dymond, J., and M. Lyle, Particle fluxes in the ocean and implications for sources and preservation of ocean sediments, in Geomaterial Fluxes, Glacial to Recent, edited by W. W. Hay, National Research Council, National Academy of Science, Washington D. C., in press, 1992.

Dymond, J., E. Suess, and M. Lyle, Barium in deep sea sediments: A geochemical indicator of paleoproductivity, Paleoceanography, 7, 163-181, 1992.

Emerson, S. E. Organic carbon preservation in marine sediments, in The Carbon Cycle and Atmospheric CO2: Natural Variations Archean to Present.Geophys. Monogr. Ser., vol. 32, edited by E. T. Sundquist and W. S. Broecke, pp. 78-89,AGU, Washington D.C., 1985.

Eppley, R. W., and B. J. Peterson, Particulate organic matter flux and planktonic new production in the deep ocean, Nature, 282, 677-680, 1979.

Farrell, J. W., and W. L. Prell, Climatic change and $CaCO_3$ preservation: An 800,000 year bathymetric reconstruction from the central equatorial Pacific Ocean, Paleoceanography, 4, 447-466, 1989.

Finney, B. P., M. W. Lyle, and G. R. Heath, Sedimentation at MANOP Site H (eastern equatorial Pacific) over the past 400,000 years: Climatically induced redox variations and their effects on transition metal cycling, Paleoceanography, 3, 169-189, 1988.

Goldberg, E. D., and G. O. S. Arrhenius, Chemistry of Pacific pelagic sediments, Geochim. Cosmochim. Acta, 13, 153-212, 1958.

Hedges, J. I., and D. C. Mann, The lignin geochemistry of marine sediments from the southern Washington coast, Geochim. Cosmochim. Acta, 43, 1809-1818, 1979.

Hedges, J. I., H. J. Turin, and J. R. Ertel, Sources and distributions of sedimentary organic matter in the Columbia River drainage basin, Washington and Oregon, Limnol. Oceanogr., 29, 35-46, 1984.

Henrichs, S. A., and W. S. Reeburgh, Anaerobic mineralization of marine sediment organic matter: Rates and the role of anaerobic processes in the oceanic carbon economy. Geomicrobiol. J., 5, 191-237, 1987.

Hickey, B. M., The California Current System - Hypotheses and facts, Progr. Oceanogr., 8: 191-279, 1979.

Huyer, J., Coastal upwelling in the California Current System, Progr. Oceanogr., 12: 259-284, 1983.

Huyer, A., P. M. Kosro, J. Fleischbein, S.R. Ramp, T. Stanton, L. Washburn, F.P. Chavez, T.J. Cowles, S.D. Pierce, and R.L. Smith, Currents and water masses of the coastal transition zone off northern California, June to August 1988. J. Geophys. Res., 96, 14809-14831,1991.

Ikeda M., and W. J. Emery, Satellite observations and modeling of meanders in the California Current system off Oregon and northern California, J. Phys. Oceanog.,14, 1434-1450, 1984.

Jahnke, R. A., Early diagenesis and recycling of biogenic debris at tha seafloor, Santa Monica Basin, California, J. Mar. Res., 48, 413-436, 1990.

Karlin, R., Sediment sources and clay mineral distributions off the Oregon coast, J. Sedimentol. Petrol., 50, 543-560 1980.

Karlin, R., and S. Levi , Geochemical and sedimentological control of the magnetic properties of hemipelagic sediments, J. Geophys. Res., 90, 10,373-10,392, 1985.

Karlin, R., and M. Lyle, Sediment Studies on the Gorda Ridge, Tech. Rep. 86-14, Oregon State Univ., Coll. of Oceanogr., Corvallis, 1986.

Karlin, R., M. Lyle, and R. Zahn, Carbonate variations in the NE Pacific during the Late Quaternary, Paleoceanography, 7, 43-63, 1992.

Kutzbach, J. E., Model simulations of the climatic patterns during the deglaciation of North America, in North America and Adjacent Oceans During the Last Deglaciation, Decade of North American Geology, vol. K-3, edited by W. F. Ruddiman and H. E. Wright, Jr., pp. 425-447, Geological Society of America, Boulder, Colo., 1987.

Landry, M. R., J. R. Postel, W. K. Peterson, and J. Newman, Broad-scale distributional patterns of hydrographic variables on the Washington/Oregon shelf, in Coastal Oceanography of Washington and Oregon, edited by M. R. Landry and B. M. Hickey, pp. 1-40, Elsevier, New York, 1989.

Laul, J. C., Neutron activation analysis of geologic materials, At. Energy Rev., 17, 603-695,1979.

Lyle, M., The brown-green color transition in marine sediments: A marker of the Fe(III)-Fe(II) redox boundary,Limnol. Oceanogr., 28, 1026-1033, 1983.

Lyle, M., Climatically forced organic carbon burial in equatorial Atlantic and Pacific oceans, Nature, 335, 529-532, 1988 .

Lyle, M., D. W. Murray, B. P. Finney, J. Dymond, J. M. Robbins, and K. Brooksforce, The record of Late Pleistocene biogenic sedimentation in the eastern tropical Pacific Ocean, Paleoceanography, 3, 39-59, 1988.

Lynn , R. J., and J. J.Simpson, The California Current system: The seasonal variability of its physical characteristics, J. Geophys. Res., 12,947-12,967, 1987.

Martin, J. H, Glacial-interglacial CO_2 change: The iron hypothesis, Paleoceanography, 5, 1-15, 1990.

Martinson, D. G., N. G. Pisias, J. D. Hays, J. Imbrie, T. C. Moore, Jr., and N. J. Shackleton Age dating and orbital theory of the ice ages: Development of a high-resolution 0 to 300,000 year chronostratigraphy. Quat. Res., 27, 1-29, 1987.

Miller, C. B., K. L. Denman, A. E. Gargett, D. L. Mackas, P. A. Wheeler, B. C. Booth, B. W. Frost, M. R. Landry, J. Lewin, C. J. Lorenzen, M. J. Perry, M. Dagg, and N. Welshmeyer, Lower trophic level production dynamics in the oceanic subarctic Pacific Bull. 26, pp.1-26, Ocean Research Inst., Univ. of Tokyo, 1988.

Moore, T. C., Jr., Late Pleistocene-Holocene oceanographic changes in the northeastern Pacific, Quat. Res., 3, 99-109, 1973.

Müller, P. J., and E. Suess, Productivity, sedimentation rate, and sedimentary organic matter in the oceans, I, Organic carbon preservation, Deep Sea Res., Part A, 26, 1347-1362, 1979.

Nelson, C. S. Wind stress and wind stress curl over the California Current. NOAA Tech. Rep., NMFS SSRF, 714, 1977.

Pares-Sierra, A., and J. J. O'Brien The seasonal and interannual variability of the California Current system: A numerical model, J. Geophys. Res., 94, 3159-3181, 1989.

Prahl, F., and L. A. Muehlhausen, Lipid biomarkers as geochemical tools for paleoceanographic study, in Productivity of the Ocean: Present and Past, John Wiley, edited by W. H. Berger et al., pp. 271-289, New York, 1989.

Prahl, F., L. Muehlhausen, and M. Lyle, An organic geochemical assessment of oceanographic conditions at MANOP Site C over the past 26,000 years, Paleoceanography, 4, 495-510, 1989a.

Prahl, F.G., G.J. de Lange, M. Lyle, and M.A. Sparrow, Post-depositional stability of long-chain alkenones under contrasting redox conditions, Nature, 341, 434-437, 1989b.

Rabouille, C., and J.-F. Gaillard, A coupled model representing the deep-sea organic carbon mineralization and oxygen consumption in surficial sediments, J. Geophys. Res., 96, 2761-2776, 1991.

Rau, G. H., P. N. Froelich, T. Takahashi, and D. J. Des Marais, Does sedimentary $\delta^{13}C$ record variations in Quaternary ocean [CO2(aq)]?, Paleoceanography, 6, 335-349, 1991a.

Rau, G. H., T. Takahashi, D. J. Des Marais, and C. W. Sullivan, Particulate organic matter $\delta^{13}C$ variations across the Drake Passage.

Riddihough, R. P. Gorda Plate motions from magnetic anomaly analysis. Earth Planet. Sci. Lett., 51, 163-170, 1980.

Riley, G. A., The relationship of vertical turbulence and spring diatom flowerings, J. Mar. Res., 5, 67-87, 1942.

Sancetta, C., M. Lyle, L. Heusser, and R. Zahn, Late Glacial to Holocene changes in upwelling and seasonal production of the northern California Current system, Quat. Res.,in press, 1992.

Sarnthein, M., K. Winn, J. C. Duplessy, and M.R. Fontugne,Global variations of surface ocean productivity in low- and mid-latitudes: Influence on CO2 reservoirs of the deep ocan and atmosphere during the last 21,000 years, Paleoceanography, 3, 361-399, 1988.

Shackleton, N. J., Attainment of isotopic equilibrium between ocean water and the benthonic foraminiferal genus Uvigerina: Isotopic changes in the ocean during the last glacial, Colloques Int. CNRS, 219, 203-219, 1974.

Shackleton, N. J., and N. G. Pisias Atmospheric carbon dioxide, orbital forcing, and climate, in The Carbon Cycle and Atmospheric CO_2: Natural Variations Archean to Present, Geophys. Monogr. Ser., vol. 32, AGU, Washington,
D. C., edited by E. T. Sundquist and W. S. Broecker, pp. 303-317, 1985.

Southon, J.R., D.E. Nelson, and J.S. Vogel (1990) A record of past ocean-atmosphere radiocarbon differences from the northeast Pacific. Paleoceanography, 5, 197-206.

Stoddard, P. R., A kinematic model for the evolution of the Gorda Plate, J. Geophys. Res., 92, 11,524-11,532, 1987.

Sverdrup, H. U., M. W. Johnson, and R. H. Fleming, The Oceans, pp. 712-730, Prentice-Hall, Englewood Cliffs, N. J., 1942.

Thomas, A. C., and P. T. Strub, Interannual variability in phytoplankton pigment distribution during the spring transition along the west coast of North America, J. Geophys. Res., 94, 18,095-18,117, 1989.

Weliky, K., E. Suess, C. A. Ungerer, P. J. Müller, and K. Fischer, Problems with accurate carbon measurements in marine sediments: A new approach, Limnol. Oceanogr., 28, 1252-1259, 1983.

Welling, L. A., Radiolarian microfauna in the northern California Current system: Spatial and temporal variability and implications for paleoceanographic reconstructions, M.S.c. thesis, 80 pp., Oregon State University, Corvallis, 1991.

Zahn, R., T. F. Pedersen, B. D. Bornhold, and A. C. Mix, Water mass conversion in the glacial Subarctic Pacific (54°N, 148°W): Physical constraints and the benthic-planktonic stable isotope record, Paleoceanography, 6, 543-561, 1991.

Zahn, R., N. Pisias, Ahmed-Rushdie, B. Bornhold, B. Blaise, and R. Karlin, Carbonate deposition and benthic δC-13 in the northeast Pacific and Pacific-Atlantic comparison: Implication for changes in the oceans' carbonate system during the last 750,000 years, Earth Planet. Sci. Lett., in press, 1992.

R. Collier, J. Dymond, N. Pisias, and F. Prahl, College of Oceanography, Oregon State University, Corvallis, OR 97331.

M. Lyle, Borehole Research Group, Lamont-Doherty Geological Observatory, Palisades, NY 10964.

E. Seuss and R. Zahn, GEOMAR, Wischhofstrasse 1-3, Giebäude 4, D-2300 Kiel 14, Germany.

(Received April 16, 1991;
revised March 4, 1992;
accepted March 20, 1992.)